Quasiclassical trajectory calculations of correlated product distributions for the $F+CHD_3(v_1=0,1)$ reactions using an *ab initio* potential energy surface

Gábor Czakó[a] and Joel M. Bowman[b]
Department of Chemistry and Cherry L. Emerson Center for Scientific Computation, Emory University, Atlanta, Georgia 30322, USA

(Received 17 November 2009; accepted 3 December 2009; published online 23 December 2009)

We report quasiclassical trajectory (QCT) calculations of the correlated product distributions and branching ratios of the reactions $F+CHD_3(v_1=0,1)\rightarrow HF(v)+CD_3(v)$ and $DF(v)+CHD_2(v)$ using a recently published *ab initio*-based full-dimensional global potential energy surface [G. Czakó *et al.*, J. Chem. Phys. **130**, 084301 (2009)]. Harmonic normal mode analysis is done for the methyl products to determine the classical actions of each normal mode and then standard histogram binning and Gaussian binning (GB) methods are employed to obtain quantum state-resolved probabilities of the products. QCT calculations have been performed for both the vibrationally ground state and the CH stretching excited $F+CHD_3(v_1=0,1)$ reactions at eight different collision energies in the 0.5–7.0 kcal/mol range. HF and DF vibrationally state-resolved rotational and angular distributions, CD_3 and CHD_2 mode-specific vibrational distributions, and correlated vibrationally state-specific distributions for the product pairs have been obtained and the correlated results were compared to the experiment. We find that the use of GB can be advantageous especially in the threshold regions. The CH stretching excitation in the reactant does not change the CD_3 vibrational distributions significantly, whereas the HF molecules become vibrationally and rotationally hotter. On the other hand in the case of the $DF+CHD_2$ channel the initially excited CH stretch appears mainly "intact" in the CHD_2 product and the DF distributions are virtually the same as formed from the ground state CHD_3 reaction. The computed results qualitatively agree with recent crossed molecular beam experiment [W. Zhang *et al.*, Science **325**, 303 (2009)] that (a) $CHD_2(v_1=1)$ is the most populated product state of the $F+CHD_3(v_1=1)$ reaction and this reaction produces much less $CHD_2(v=0)$ compared to the reaction $F+CHD_3(v=0)$; (b) the cross section ratio of $CHD_2(v_1=1):CHD_2(v=0)$ formed from the reactions $F+CHD_3(v_1=1):F+CHD_3(v=0)$ is less than 1 and shows little collision energy dependency; (c) the reactant CH stretch excitation increases the DF:HF ratio at low collision energies; (d) the correlated vibrational and angular distributions for $DF(v)+CHD_2(v_1=0,1)$ from the ground state and stretch-excited reactions, respectively, are almost identical. © *2009 American Institute of Physics*. [doi:10.1063/1.3276633]

I. INTRODUCTION

Bimolecular chemical reactions play a central role in chemistry; therefore, one wants to understand the fundamental details that govern these reactions. One of the fundamental rules is the Polanyi rule,[1] which predicts that the reactant vibrational excitations promote the reaction if the transition state has a product-like structure (late barrier), whereas the translation energy drives the early barrier reactions more effectively. This rule works well in the case of atom+diatom reactions; however, little has been known about the validity of the extension of this simple picture for polyatomic reactions, especially for reactions involving molecules with more than three atoms. A few experimental groups probed the effect of the CH stretch excitation for the late barrier $Cl+CH_4(v_1=0,1)$ reaction, i.e., Crim *et al.*[2,3] ($Cl+CH_3D$), Liu *et al.*[4] ($Cl+CHD_3$), and Zare *et al.*[5,6] ($Cl+CH_2D_2$ and $Cl+CH_4$). Unexpectedly, Liu and co-workers[4] found that the translational energy is more effective to activate the $Cl+CHD_3$ reaction than the reactant CH stretching excitation, in contradiction to the Polanyi rule. Furthermore, a recent experiment on the early barrier $F+CHD_3(v_1=0,1)$ reaction showed that the CH stretching excitation inhibits the break of the CH bond.[7] Therefore, the mode-selective dynamics of polyatomic reactions is far from being well understood and the recent experiments "highlight substantial gaps in our predictive framework for state-selective polyatomic reactivity."[7]

Classical molecular dynamics calculations are frequently used in order to describe the nuclear dynamics of chemical reactions. For applications in the gas phase initial coordinates and velocities are chosen for the reactants, which correspond to quantum mechanical (ro-)vibrational energy levels. The trajectories, initialized in these quasiclassical (ro-)vibrational states, are known as quasiclassical trajectories (QCTs). They are obtained by propagating the classical equations of motion while the required forces, i.e., potential gradients, are computed quantum mechanically. Based on the

[a]Electronic mail: czako@chem.elte.hu.
[b]Electronic mail: jmbowma@emory.edu.

final coordinates and velocities one is often interested in computing the (ro-)vibrational distributions of the product molecules, which requires "quantum number" assignment for the products. This is straightforward for diatomic molecules since they have only one vibrational degree of freedom; thus obviously the total vibrational energy corresponds to the single mode. Therefore, QCT has been used for the $A+BC \rightarrow AB(v,J)+C$ reactions and the computed AB (ro-)vibrational distributions sometimes had excellent agreement with quantum simulations and/or experiments.[8] These atom+diatom reactions can also be studied by quantum dynamics; however, for polyatomic reactions the quantum treatment of the nuclear motion is computationally not feasible currently; thus, one should calculate (ro-)vibrational state distributions for polyatomic product molecules from QCT calculations. The recent experiments of Liu and co-workers[7,9–12] on the $F+CH_4 \rightarrow HF(v)+CH_3(v)$ reaction and its isotope substituted analogs add to our motivation to develop vibrational quantum number assignment for polyatomic products since they measured the vibrationally state-specific correlation of coincident product pairs in the above-mentioned reactions.

There have been many QCT and several experimental studies of the $F+CH_4 \rightarrow HF+CH_3$ reaction.[13–19] Most of them were reviewed in our recent paper (see Ref. 20), where we reported an accurate *ab initio* full-dimensional potential energy surface (PES) for this early barrier reaction. The PES contains a first-order saddle point $(CH_4-F)_{SP}$, which is slightly above (by 240 cm^{-1}) the reactant asymptote and has a nonlinear C–H–F bond arrangement.[20] The reaction is exothermic; the best estimate for the vibrationless energy difference between products and reactants is $-10\,000$ cm^{-1} (-28.59 kcal/mol).[20] In the exit valley there is a relatively stable, $D_e=1070$ cm^{-1}, van der Waals (vdW) complex $(CH_3-HF)_{vdW}$ having C_{3v} point-group symmetry. For the diatomic HF product of the $F+CH_4$ reaction the rotational-vibrational distributions were computed recently[20] and we found excellent agreement with the experiment.[19] However, we did not analyze the vibrationally state-resolved populations of the polyatomic methyl product in that paper.[20]

In the present paper we focus on the $F+CHD_3(v_1=0,1)$ reactions, which have been the subject of experiments performed by Liu and co-workers.[7,11] Recently, QCT calculations using a semiempirical PES have also been carried out for the $F+CHD_3(v=0)$ reaction by Espinosa-García.[21,22] This reaction has two major product channels, $HF(v)+CD_3(v)$ and $DF(v)+CHD_2(v)$. In previous experiments the collisions of ground state reactants were studied and the HF/DF vibrational distributions were correlated with the ground state CD_3/CHD_2 products.[11] In the most recent experiment the effect of the reactant CH symmetric stretching mode, $v_1(a_1)$, excitation has been studied by measuring the correlated vibrationally state-specific product pair distributions.[7] This recent experiment found that the CH stretching excitation inhibits the break of the CH bond, and thus promotes the $DF+CHD_2$ product channel.[7] We have recently investigated this unexpected effect theoretically and our QCT calculations have shown that the CH stretching excitation steers the F atom to the CD bond at low collision energies (for more details see Ref. 23); thus, this stereodynamical effect explains the surprising experimental finding.

In order to simulate the interesting correlated experimental distributions we apply a method for normal mode quantum number assignment for polyatomic products. In Sec. II this procedure is described in a general context and in Sec. IV we apply this method for the CD_3 and CHD_2 products of the $F+CHD_3(v_1=0,1)$ reactions correlated with the corresponding diatomic product. We also describe how we have verified that QCT with normal mode sampling[24] can be used for studying mode selective chemistry. In Sec. III we briefly review the computational details of the *ab initio* PES (Ref. 20) employed in this study. The vibrational frequencies corresponding to the saddle point, exit channel vdW complex, and the products of the $F+CHD_3$ reaction are also given and the fully anharmonic energy levels are compared to the available experimental results. The QCT results including HF/DF vibrationally state-resolved rotational and angular distributions, CD_3 and CHD_2 vibrational distributions, and correlated vibrationally state-specific product pair distributions are reported in Sec. IV, where we also compare the computed results to the recent cross molecular beam experiments.[7,11] The paper ends with summary and conclusions (Sec. V).

II. NORMAL MODE QUANTUM NUMBER ASSIGNMENT FOR POLYATOMIC PRODUCTS

The assignment of quantum states for polyatomic products is closely related to the semiclassical quantization of polyatomic molecules, a topic of considerable interest over that past 30 years.[25] In the present context the goal is more modest, namely, to determine the harmonic actions of the polyatomic products. Espinosa-García[18,21,22] briefly described a procedure to do this and we give the details of how we obtain harmonic classical actions for the polyatomic products.

Let us consider a polyatomic product molecule with N nuclei, whose final Cartesian coordinates and corresponding velocities in the center of mass frame are denoted by $\mathbf{r}_i$ and $\mathbf{v}_i$ $(i=1,2,\ldots,N)$, respectively. First we determine the classical angular momentum of the product. To proceed with the normal mode analysis we find it convenient to remove this angular momentum using the standard modification to the velocities

$$\mathbf{v}_i^{\mathrm{nr}} = \mathbf{v}_i - \mathbf{\Omega}_i \times \mathbf{r}_i, \tag{1}$$

where the angular velocity $\mathbf{\Omega}_i$ can be obtained as

$$\mathbf{\Omega}_i = \mathbf{I}^{-1}\mathbf{j}_i, \tag{2}$$

where $\mathbf{I}^{-1}$ is the inverse of the moment of inertia tensor corresponding to geometry $\mathbf{r}_i$ and $\mathbf{j}_i=\mathbf{r}_i\times(m_i\mathbf{v}_i)$, where m_i denotes the mass of the ith atom.

Since the product molecule configuration is generally not at a stationary point, we need to relate the actual configuration to normal mode displacements of a reference minimum geometry. Our approach is to determine this reference geometry as follows. Starting at the given configuration, we use a gradient-based method to locate the equilibrium structure (denoted as $\mathbf{r}_i^{\mathrm{eq}}$). In principle this method does not trans-

late the center of mass nor rotate the axis system, and in most cases, because the starting configuration is not highly distorted from the equilibrium structure, this geometry can be found within a few steps. After the optimization is completed we do check that the Eckart conditions[26]

$$\sum_{i=1}^{N} m_i \Delta \mathbf{r}_i = \mathbf{0} \tag{3}$$

and

$$\sum_{i=1}^{N} m_i \mathbf{r}_i^{\mathrm{eq}} \times \Delta \mathbf{r}_i = \mathbf{0} \tag{4}$$

are satisfied, where $\Delta \mathbf{r}_i = \mathbf{r}_i - \mathbf{r}_i^{\mathrm{eq}}$. In actual calculations these equations are of course not exactly satisfied and so final, generally small adjustments [e.g., $\mathbf{r}_i^{\mathrm{eq}}$ is moved to the center of mass frame if Eq. (3) is not exactly satisfied] to the coordinate system are done to satisfy these conditions. In the case of the CD_3/CHD_2 product molecules, if we minimize the expression

$$\left\| \sum_{i=1}^{N} m_i \mathbf{C}\mathbf{r}_i^{\mathrm{eq}} \times (\mathbf{r}_i - \mathbf{C}\mathbf{r}_i^{\mathrm{eq}}) \right\| \tag{5}$$

with respect to the three Euler angles, where $\mathbf{C}$ is an orthogonal rotational matrix depending on the Euler angles, the rotation angles are either essentially numerically zero, i.e., no adjustment is needed, or less than 1.5°. Therefore, we can say that a gradient-based optimization starting from the final coordinates of the polyatomic product finds the numerically optimal orientation of the equilibrium structure. Although we did minimize the cross product of Eq. (5) in our QCT study, but as preliminary test calculations showed, neglecting this step would not compromise the final results significantly.

Having determined the relevant reference geometry, we perform a normal mode analysis there, which provides, in the case of nonlinear equilibrium structure, $3N-6$ nonzero harmonic frequencies ω_k and the orthogonal transformation matrix $\mathbf{l} \in \Re^{(3N-6)\times 3\times N}$, which transforms from mass-scaled Cartesian coordinates to normal coordinates. Thus, the normal coordinates can be obtained as

$$Q_k = \sum_{i=1}^{N} \sqrt{m_i} \mathbf{l}_{ki} \Delta \mathbf{r}_i, \quad k = 1,2,\ldots,3N-6 \tag{6}$$

and similarly the momenta in the normal coordinate space are

$$P_k = \sum_{i=1}^{N} \sqrt{m_i} \mathbf{l}_{ki} \mathbf{v}_i^{\mathrm{nr}}, \quad k = 1,2,\ldots,3N-6. \tag{7}$$

Employing these normal coordinates and momenta the vibrational energy for each normal mode can be calculated as

$$E_k = \frac{P_k^2}{2} + \frac{\omega_k^2 Q_k^2}{2}, \quad k = 1,2,\ldots,3N-6. \tag{8}$$

Thus, a noninteger classical harmonic action number for each mode can be obtained as

$$n_k' = \frac{E_k}{\omega_k} - \frac{1}{2}, \quad k = 1,2,\ldots,3N-6. \tag{9}$$

The integer vibrational quanta can be assigned to quantum states by rounding n_k' to the nearest integer value n_k. Hereafter we denote a vibrational state $(n_1, n_2, \ldots, n_{3N-6})$ as $\mathbf{n}$. In what follows we describe how the vibrationally state-resolved probabilities can be computed for the polyatomic products.

A. Histogram binning

If the number of the products in a particular vibrational state $\mathbf{n}$ is $N(\mathbf{n})$ from the total number of trajectories N_{traj}, the widely used histogram binning (HB) gives that the probability of the state $\mathbf{n}$ is

$$P_{\mathrm{HB}}(\mathbf{n}) = \frac{N(\mathbf{n})}{N_{\mathrm{traj}}}. \tag{10}$$

Since we obtained $\mathbf{n}$ by rounding the noninteger classical action numbers, $\mathbf{n}$ can be an energetically closed state, a well-known issue of HB.

B. Gaussian binning

In order to get a more realistic energetic description of the reaction the so-called Gaussian binning (GB) method has been proposed in the QCT calculations.[27–30,8] In this approach a Gaussian weight is calculated for each product. Here we consider two strategies to calculate the weight for a polyatomic product. In the first approach a weight for each normal mode of the pth product in a given vibrational state $\mathbf{n}$ is calculated as

$$G_p(n_k) = \frac{\beta}{\sqrt{\pi}} e^{-\beta^2 (n_{k,p}' - n_k)^2}, \quad p = 1,2,\ldots,N(\mathbf{n}), \tag{11}$$

where β is a positive real parameter. If the full width at half maximum is δ, $\beta = 2\sqrt{\ln 2}/\delta$. Thus, the weight for a vibrational state of an N-atomic molecule is

$$G_p(\mathbf{n}) = \prod_{k=1}^{3N-6} G_p(n_k), \quad p = 1,2,\ldots,N(\mathbf{n}). \tag{12}$$

This approach, however, needs an extremely large number of trajectories for statistical accuracy comparable to HB. Furthermore, the number of required trajectories increases rapidly with increasing number of vibrational modes. Therefore, we also propose another approach, where the weight is obtained as

$$G_p(\mathbf{n}) = \frac{\beta}{\sqrt{\pi}} e^{-\beta^2 ([E(\mathbf{n}_p') - E(\mathbf{n})]/[2E(\mathbf{0})]^2}, \quad p = 1,2,\ldots,N(\mathbf{n}), \tag{13}$$

where $E(\mathbf{0})$ is the harmonic zero-point vibrational energy (ZPVE) and

$$E(\mathbf{n}_p') = \sum_{k=1}^{3N-6} \omega_k \left(n_{k,p}' + \frac{1}{2} \right)$$

and

TABLE I. ZPVEs and all the fundamentals (in cm^{-1}) for CHD_3 and the saddle point $(D_3CH-F)_{SP}$ and $(D_2HCD-F)_{SP}$ (see Fig. 1 for the structures).

CHD_3 (C_{3v})				$(D_3CH-F)_{SP}$ (C_s)		$(D_2HCD-F)_{SP}$ (C_s)	$(D_2HCD-F)_{SP}$ (C_1)
	ω [a]	v [b]	Expt.[c]		ω [a]	ω [a]	ω [a]
ZPVE	7850(7880)	7757		$ZPVE_{SP}$	7634(7681)	7740(7654)	7749(7711)
				ω_{12}	317*i*(240*i*)	309*i*(264*i*)	284*i*(239*i*)
				ω_{11}	33(139)	30(29)	31(86)
				ω_{10}	103(142)	100(62)	103(92)
$v_3(a_1)$	1013(1029)	996	1003	ω_9	1008(1007)	969(968)	978(979)
$v_6(e)$	1046(1059)	1030	1036	ω_8	1076(1062)	1005(989)	1021(1001)
				ω_7	1076(1064)	1071(1049)	1068(1051)
$v_5(e)$	1316(1325)	1287	1291	ω_6	1212(1226)	1300(1280)	1269(1260)
				ω_5	1230(1238)	1331(1312)	1343(1324)
$v_2(a_1)$	2187(2185)	2136	2142	ω_4	2192(2189)	**1903(1893)**	**1904(1894)**
$v_4(e)$	2328(2329)	2244	2263	ω_3	2360(2347)	2261(2249)	2251(2246)
				ω_2	2375(2350)	2375(2350)	2364(2346)
$v_1(a_1)$	3120(3120)	2985	2993	ω_1	**2603(2598)**	3137(3127)	3167(3142)

[a]Harmonic frequencies corresponding to the PES, while the frozen-core UCCSD(T)/aug-cc-pVTZ *ab initio* results are given in parenthesis. In the case of the saddle point frequencies, especially for the low-lying ones, the *ab initio* values have significant uncertainties due to uncertainties in the numerical Hessian calculation. The bold redshifted frequencies indicate the product channel of the $F+CHD_3$ reaction.
[b]VCI energies were computed with 4MRs using the $[7_7 6_7 5_7 3_6 2_6]$ basis of 6406 functions.
[c]Experimental levels for CHD_3 were taken from Ref. 40.

$$E(\mathbf{n}) = \sum_{k=1}^{3N-6} \omega_k \left(n_k + \frac{1}{2} \right), \tag{14}$$

where $\mathbf{n}$ is the quantum state assigned using HB. Note that employing these definitions the following relation holds:

$$-0.5 \leq \frac{E(\mathbf{n}_p') - E(\mathbf{n})}{2E(\mathbf{0})} < 0.5. \tag{15}$$

Employing the GB using either Eq. (12) or Eq. (13) the probability of the vibrational state $\mathbf{n}$ can be obtained as

$$P_{GB}(\mathbf{n}) = \frac{\Sigma_{p=1}^{N(\mathbf{n})} G_p(\mathbf{n})}{N_{traj}}. \tag{16}$$

Note that GB [Eq. (16)] becomes HB [Eq. (10)] if $G_p(\mathbf{n}) \equiv 1$ for $p=1,2,\ldots,N(\mathbf{n})$. Details about the implementation of these binning methods for the CD_3 and CHD_2 products of the $F+CHD_3$ reaction are given in Sec. IV B 1.

III. VIBRATIONAL DYNAMICS ON THE POTENTIAL ENERGY SURFACE

A. Potential energy surface

Recently, an accurate full-dimensional global PES for the $F+CH_4 \rightarrow HF+CH_3$ reaction has been developed in our group based on *ab initio* energy points obtained by an efficient composite method (see Ref. 20). These composite energies, i.e., 12 384 data points in the complex region (FCH_4), were obtained from the expression $E_{UCCSD(T)/aVDZ} + E_{UMP2/aVTZ} - E_{UMP2/aVDZ}$, where the energies were computed at the frozen-core UHF-UCCSD(T)/aug-cc-pVDZ, UMP2/aug-cc-pVTZ, and UMP2/aug-cc-pVDZ levels of theory, respectively. Our detailed test computations showed that this composite approach performs almost as well as the computationally much more expensive UCCSD(T)/aug-cc-pVTZ level. Furthermore, 7000 configurations were added from fragment data: 2000 for CH_4+F, 2000 for CH_3+HF, 2000 for CH_2F+H_2, and 1000 for CH_3F+H. The PES is represented by a polynomial expansion in Morse-like variables of the internuclear distances and using a compact polynomial basis that is explicitly invariant under permutations of the H atoms.[31] We included all terms up to total degree 6 and the total number of free coefficients determined by a weighted linear least-squares fit is 3262. For detailed description of the PES and the highly accurate *ab initio* characterization of the stationary points, the interested reader can consult Ref. 20.

B. Vibrational energy levels relevant to the $F+CHD_3$ reaction

ZPVEs and all the fundamental frequencies for [CHD_3, $(D_3CH-F)_{SP}$, and $(D_2HCD-F)_{SP}$] and as well as for [$(CD_3-HF)_{vdW}$, CD_3, and HF] and [$(CHD_2-DF)_{vdW}$, CHD_2, and DF] are presented in Tables I–III, respectively. The harmonic frequencies correspond to the fitted PES and for comparison UCCSD(T)/aug-cc-pVTZ *ab initio* values obtained by MOLPRO (Ref. 32) are also given. For all the species, except at the saddle point, variational vibrational calculations have also been performed by the program package MULTIMODE (MM) (Refs. 33 and 34) using the vibrational configuration interaction (VCI) method. MM employs the finite basis representation of the Watson Hamiltonian[35] using the so-called *n*-mode representation[36,37] (*n*MR) for the potential and the inverse of the effective moment of inertia. The presented results were obtained by using 4MRs and the further computation details were the same as in Ref. 20. In the case of the reactant and products, the averaged absolute deviations (in cm^{-1}) between the calculated anharmonic and the available

TABLE II. ZPVEs and vibrational frequencies (in cm^{-1}) for the product vdW complex $(CD_3-HF)_{vdW}$ and the products (CD_3 and HF).

$(CD_3-HF)_{vdW}$ (C_{3v})			CD_3 (D_{3h})				HF			
	ω [a]	v [b]		ω [a]	v [b]	Expt.[c]		ω [a]	v [b]	Expt.[c]
ZPVE	7465(7384)	7418	ZPVE	4769(4793)	4737		ZPVE	2049(2062)	2033	
$\upsilon_{HF}(a_1)$	4049(3940)	3882[d]					υ_1	4098(4124)	3941	3961
$\upsilon_s(a_1)$	113(133)	123					υ_2	8196(8248)	7725	7751
$\upsilon_b(e)$	96(99)	188					υ_3	12 294(12 372)	11 354	11 373
$\upsilon_b(e)$	452(414)	532					υ_4	16 392(16 496)	14 825	14 832
$\upsilon(a_1)$	520(493)	541	$\upsilon_2(a_2'')$	394(385)	449	458				
$\upsilon(e)$	1031(1045)	1037	$\upsilon_4(e')$	1036(1044)	1021	1026				
$\upsilon(a_1)$	2203(2196)	2177	$\upsilon_1(a_1')$	2186(2203)	2139	2158				
$\upsilon(e)$	2444(2446)	2390	$\upsilon_3(e')$	2444(2455)	2366	2381				

[a]Harmonic frequencies corresponding to the PES, while the frozen-core UCCSD(T)/aug-cc-pVTZ *ab initio* results are given in parenthesis.
[b]For $(CD_3-HF)_{vdW}$ and CD_3 VCI energies were computed with 4MRs using the bases $[7_7 6_7 4_7 3_6 2_6]$ of 20 688 and $[7_7 6_7 5_7 3_6 2_6]$ of 1319 functions, respectively. In the case of HF converged anharmonic vibrational levels were obtained by a one-dimensional discrete variable representation code.
[c]Experimental levels for CD_3 and HF were taken from Refs. 41 and 42, respectively.
[d]Our best estimate for the anharmonic $\upsilon_{HF}(a_1)$ is $3940+(3882-4049)=3773$ cm^{-1}.

experimental fundamentals are 8 (CHD_3), 12 (CD_3), 6 (CHD_2), 20 (HF), and 19 (DF).

1. Saddle point for the HF+CD$_3$ and DF+CHD$_2$ channels

The saddle point $(D_3CH-F)_{SP}$ for the HF+CD_3 channel of the F+CHD_3 reaction has C_s point-group symmetry, whereas the complex $(D_2HCD-F)_{SP}$ corresponding to the DF+CHD_2 channel has either C_s (H is in the C_s plane) or C_1 (H is one of the out-of-plane atoms) symmetry (see Fig. 1). In the case of each unique arrangement of the H and the three D atoms, the saddle point has imaginary frequencies of 317*i*, 309*i*, and 284*i* cm^{-1}, respectively, corresponding to an intermolecular stretching mode between CHD_3 and F. Furthermore, each saddle point has two low-lying fundamentals—33, 30, and 31 cm^{-1} and 103, 100, and 103 cm^{-1}—which correspond to intermolecular bending modes. The other nine fundamentals correspond to the vibrational modes of the CHD_3 unit, as shown in Table I. The saddle point has bent $[C_s, C_s, C_1]$ structure depending on the unique arrangements of the H and three D atoms; therefore, all the degenerate fundamentals of CHD_3 are split as can be seen in Table I. Note that similar to the F^-–CH_4 anion complex,[38] the CH and CD (H and D are connected to F) stretching fundamentals at the saddle point are significantly redshifted by about 500 (CH) and 300 (CD), in cm^{-1}, relative to the corresponding frequencies (υ_1 and υ_2, respectively) of the free CHD_3 molecule. This redshifted band clearly indicates if the saddle point corresponds to either the HF or the DF product channel of the F+CHD_3 reaction (see Table I).

2. Van der Waals complexes for the HF+CD$_3$ and DF+CHD$_2$ channels

Variational vibrational calculations have been performed in full (12) dimensions for $(CD_3-HF)_{vdW}$ and

TABLE III. ZPVEs and vibrational frequencies (in cm^{-1}) for the product vdW complex $(CHD_2-DF)_{vdW}$ and the products (CHD_2 and DF).

$(CHD_2-DF)_{vdW}$ (C_s)			CHD_2 (C_{2v})				DF			
	ω [a]	v [b]		ω [a]	v [b]	Expt.[c]		ω [a]	v [b]	Expt.[c]
ZPVE	7386(7333)	7348	ZPVE	5350(5377)	5308		ZPVE	1485(1495)	1477	1488
$\upsilon_{DF}(a')$	2936(2858)	2862[d]					υ_1	2971(2990)	2888	2907
$\upsilon_s(a')$	107(114)	144					υ_2	5942(5980)	5694	5722
$\upsilon_b(a'')$	94(97)	186					υ_3	8913(8970)	8418	8445
$\upsilon_b(a')$	121(137)	225					υ_4	11 884(11 960)	11 060	11 078
$\upsilon_b(a'')$	329(302)	379					υ_5	14 855(14 950)	13 619	13 618
$\upsilon_b(a')$	334(308)	377								
$\upsilon(a')$	576(547)	612	$\upsilon_4(b_1)$	435(426)	504	510				
$\upsilon(a')$	1037(1052)	1045	$\upsilon_3(a_1)$	1041(1050)	1018					
$\upsilon(a'')$	1284(1302)	1283	$\upsilon_6(b_2)$	1291(1302)	1267					
$\upsilon(a')$	2275(2270)	2241	$\upsilon_2(a_1)$	2262(2278)	2205					
$\upsilon(a'')$	2444(2446)	2396	$\upsilon_5(b_2)$	2444(2455)	2368					
$\upsilon(a')$	3233(3233)	3129	$\upsilon_1(a_1)$	3227(3244)	3097					

[a]Harmonic frequencies corresponding to the PES, while the frozen-core UCCSD(T)/aug-cc-pVTZ *ab initio* results are given in parenthesis.
[b]For $(CHD_2-DF)_{vdW}$ and CHD_2 VCI energies were computed with 4MRs using the bases $[7_7 6_7 4_7 3_6 2_6]$ of 20 688 and $[7_7 6_7 5_7 3_6 2_6]$ of 1319 functions, respectively. In the case of DF converged anharmonic vibrational levels were obtained by a one-dimensional discrete variable representation code.
[c]Experimental levels for CHD_2 and DF were taken from Refs. 41 and 43, respectively. For DF the $G(v)=\omega_e(v+1/2)-\omega_e x_e(v+1/2)^2$ formula was used, where $\omega_e=2998.19$ and $\omega_e x_e=45.76$ cm^{-1} obtained from the measured bands υ_1 and υ_2.
[d]Our best estimate for the anharmonic $\upsilon_{DF}(a')$ is $2858+(2862-2936)=2784$ cm^{-1}.

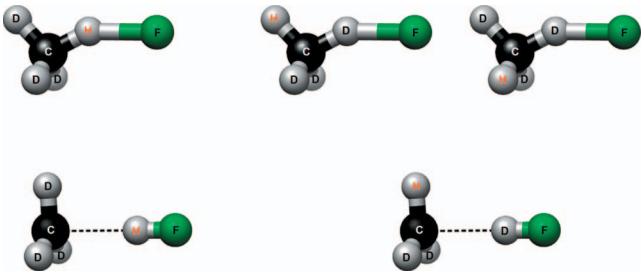

FIG. 1. Structures of $(D_3CH-F)_{SP}$ (C_s symmetry) and $(D_2HCD-F)_{SP}$ (C_s and C_1 symmetry) (upper figures) as well as $(CD_3-HF)_{vdW}$ (C_{3v} symmetry) and $(CHD_2-DF)_{vdW}$ (C_s symmetry) (lower figures).

$(CHD_2-DF)_{vdW}$. Since these complexes are weakly bonded floppy systems, several MM computations have been carried out in order to check the convergence of the vibrational energy levels. The convergence properties were similar to that of Ref. 20; therefore, the details are not repeated here. The final results reported in Tables II and III have been obtained by 4MRs and a basis of 20 688 functions. Note that the 4MR energies agreed with the 5MR ones within 1 cm^{-1} on average.

Since the vdW complexes are composed of weakly interacting CD_3/CHD_2 and HF/DF molecules, 7 (6+1) of the 12 fundamentals of the complexes correspond to the frequencies of the monomers. Perhaps the most interesting mode is the HF stretching of the complex, which was measured in the cases of $(CH_3-HF)_{vdW}$ and $(CD_3-HF)_{vdW}$ by infrared laser spectroscopy in helium nanodroplets.[39] For the HF fundamental of $(CD_3-HF)_{vdW}$ our best estimate is 3940 $+(3882-4049)=3773$ cm^{-1}, based on the UCCSD(T)/aug-cc-pVTZ *ab initio* harmonic frequency (3940 cm^{-1}) and the anharmonicity (in parenthesis) calculated using the MM result (3882 cm^{-1}) and the harmonic frequency (4049 cm^{-1}) corresponding to the PES. This computed band of 3773 cm^{-1} is in good agreement with experiment (3787 cm^{-1}). In a previous study[20] we obtained 3786 cm^{-1} for the HF band in the $(CH_3-HF)_{vdW}$ complex. The HF stretching fundamental of both $(CH_3-HF)_{vdW}$ and $(CD_3-HF)_{vdW}$ are significantly redshifted relative to the vibrational fundamental of the HF monomer (3941 cm^{-1}) and the computed (experimental) HF stretch of $(CD_3-HF)_{vdW}$ has a larger redshift by 13(10) cm^{-1} than the corresponding band in $(CH_3-HF)_{vdW}$.

For the $DF+CHD_2$ exit channel complex, i.e., $(CHD_2-DF)_{vdW}$, the DF band has not been measured. Our computed DF frequency for this complex is 2858 $+(2862-2936)=2784$ cm^{-1}, whereas the variationally computed fundamental of the DF monomer is 2888 cm^{-1}.

IV. QUASICLASSICAL TRAJECTORY CALCULATIONS

QCT calculations have been performed using the PES of Ref. 20 in order to study the dynamics of the ground state reaction, i.e., $F+CHD_3(v=0)$, and the CH stretching excited reaction, i.e., $F+CHD_3(v_1=1)$. The quasiclassical $v=0$ and $v_1=1$ states of the reactant CHD_3 were set by randomly sampling the normal coordinates and momenta,[24] while the energy for each mode was constrained at $\omega_k/2$ $(k=1,\ldots,9)$ and $[3\omega_1/2,\ \omega_k/2\ (k=2,\ldots,9)]$ for the ground and CH stretching excited states, respectively. Note that here we have used separate indexes for the degenerate modes and $\Sigma_{k=1}^{9}\omega_k/2=7850$ cm^{-1}, whereas the harmonic frequency of the CH stretching mode is $\omega_1=3120$ cm^{-1}. The angular momentum of CHD_3 was always set to zero by employing standard adjustment of the velocities. The initial distance of the F atom from the center of the mass of the CHD_3 molecule was $\sqrt{x^2+b^2}$, where b is the impact parameter and x was set to 10 bohr. The orientation of CHD_3 was randomly sampled with respect to the F atom and b was scanned from 0 to b_{max} with a step size of 0.125 bohr. Trajectories were computed at eight different collision energies (0.5, 1.0, 1.8, 2.8, 4.0, 5.0, 6.0, and 7.0 kcal/mol) for both reactions. The employed b_{max} values were 7 bohr (57 different b parameters) in the 1.8–7.0 kcal/mol range and 9 bohr (73 different b values) at the lowest two collision energies. 5000 trajectories were computed for each b; thus the total number of trajectories is 285 000 for each collision energy in the range of 1.8–7.0 kcal/mol and 365 000 for each of the lowest two collision energies. Altogether we computed and analyzed roughly 5×10^6 trajectories for the two reactions. All the trajectories were integrated using 0.0726 fs integration step. Most of the trajectories were propagated for a maximum of 20 000 time steps (1452 fs), whereas 30 000 time steps (2178 fs) were allowed at collision energies of 0.5 and 1.0 kcal/mol.

An important issue in doing initial excitation of a polyatomic reactant in QCT calculations is the possible leakage of that excitation energy to other modes on the time scale of the collision. In order to verify that the CH stretch excitation energy does not leak to the other modes, most importantly to the CD stretching modes, we have run 100 trajectories for the free CH stretch excited $CHD_3(v_1=1)$ molecule and we have computed the normal mode classical action numbers for all the vibrational modes, employing the procedure described in Sec. II, as a function of the integration time. These noninteger quantum numbers averaged over phase space and integration time are shown in Fig. 2. The trajectories for the free $CHD_3(v_1=1)$ were propagated for 5000 time steps. Note that even at the lowest collision energies the F atom begins to interact with CHD_3 within 5000 time steps. As seen in Fig. 2 the stretching modes lose some energy whereas the bending quanta slightly increase in time. Nevertheless, the free $CHD_3(v_1=1)$ maintains its CH stretch-excited character; therefore, this test clearly shows that QCT can be used to investigate the effect of CH stretching excitation in the $F+CHD_3$ reaction.

A. Cross section ratios and diatomic product rovibrational and angular distributions

1. Binning techniques

The vibrational and rotational quantum numbers have been assigned for the products HF and DF as follows. First, the classical angular momentum j of HF/DF was calculated using the final Cartesian coordinates and velocities. The quantum number J was obtained from the quantum mechanical expression $j=\sqrt{J(J+1)}$ by rounding J to the nearest inte-

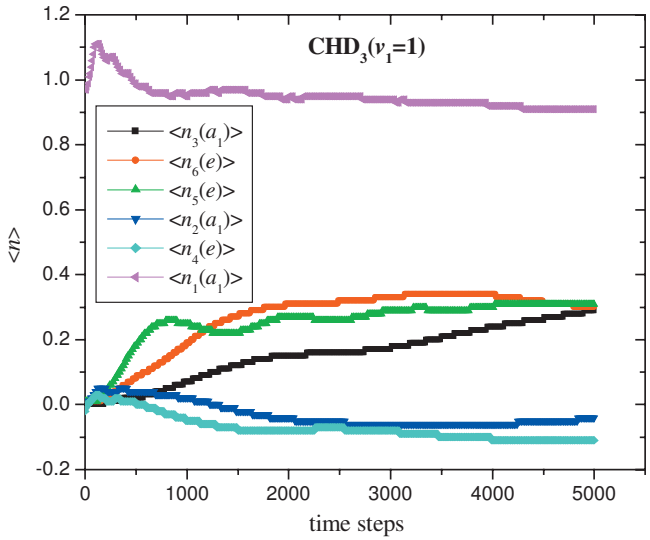

FIG. 2. Expectation values of the harmonic vibrational quanta corresponding to the normal modes of $CHD_3(v_1=1)$ as a function of integration time. A time step is 0.0726 fs and the harmonic action numbers are averaged over 100 trajectories and the time interval $[0,t]$. The initial quasiclassical CH stretching excited $v_1=1$ state of CHD_3 was set by standard normal mode sampling and the F atom was placed far, i.e., no interaction between F and $CHD_3(v_1=1)$, from the CH excited CHD_3 molecule.

ger value. Second, all the relevant rovibrational energy levels $(E_{v,J})$ of the HF and DF molecules were computed variationally using a one-dimensional cut of our global PES. The vibrational quantum number v for HF/DF was obtained by minimizing the formula $|E_{v,J}-E_{\text{int}}|$ with respect to v, where E_{int} is the internal, i.e., rovibrational, energy of the HF/DF molecule and J is the previously calculated rotational quantum number. This method corresponds to the HB for diatomic products.

We define Gaussian weights for the HF(v)/DF(v) products as

$$G(v)=\frac{\beta}{\sqrt{\pi}}e^{-\beta^2([E_{\text{int}}-E_{v,J}]/[E_{v,J}-E_{v-1,J}])^2} \quad \text{if } E_{\text{int}}<E_{v,J}, \tag{17}$$

$$G(v)=\frac{\beta}{\sqrt{\pi}}e^{-\beta^2([E_{\text{int}}-E_{v,J}]/[E_{v+1,J}-E_{v,J}])^2} \quad \text{if } E_{\text{int}}\geq E_{v,J}. \tag{18}$$

If the diatomic product violates the ZPVE, i.e., $E_{\text{int}}<E_{0,J}$, then Eq. (17) can be still used with the $E_{-1,J}=-E_{0,J}$ definition. Note that the following relations hold:

$$-0.5<\frac{E_{\text{int}}-E_{v,J}}{E_{v,J}-E_{v-1,J}}<0$$

and

$$0\leq\frac{E_{\text{int}}-E_{v,J}}{E_{v+1,J}-E_{v,J}}\leq 0.5. \tag{19}$$

Using these weights we can employ the GB(δ), where δ indicates the full width at half maximum. In this study we usually use $\delta=0.1$ for GB of HF/DF.

In the present study almost all of the product HF/DF molecules are vibrationally excited and none of them have less vibrational energy than the quantum ZPVE of HF/DF. However, the reactions, especially the ground state reaction, produce a large fraction of vibrationally ground state CD_3/CHD_2 molecules, thus, as expected, QCT can result in CD_3/CHD_2 products with less vibrational energy than ZPVE. Therefore, two sets of results are considered for the HF/DF vibrationally state-resolved distributions. One of them uses all the trajectories regardless the vibrational energy of CD_3/CHD_2 denoted as HB_{all} and $GB_{\text{all}}(\delta)$. Another set of results, denoted as HB_{ZPVE} and $GB_{\text{ZPVE}}(\delta)$, is based only on trajectories in which the CD_3/CHD_2 products have vibrational energy (internal energy after subtracting the rotational energy) at least the corresponding ZPVE.

In the case of the angular distributions standard HB was used for cos θ, where θ is the angle between the center of mass relative velocity vectors of the reactants and products, using 20 equidistant bins in the interval $[-1, 1]$.

2. DF:HF and $\sigma(v_1=1):\sigma(v=0)$ ratios

DF:HF cross section ratios in the case of both reactions as a function of collision energy are shown in Fig. 3. The cross sections are summed over the vibrational states of HF

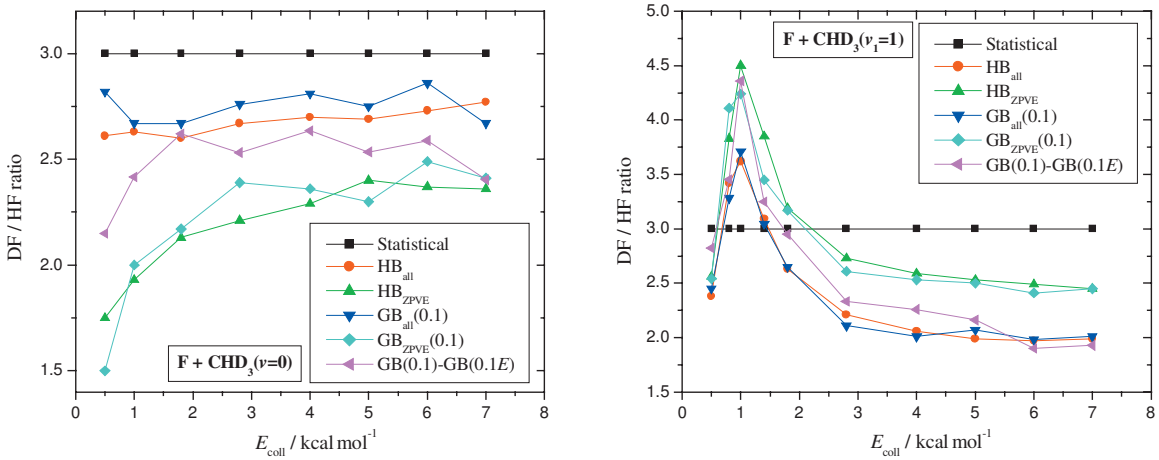

FIG. 3. Branching ratios of the DF+CHD_2 and HF+CD_3 channels of F+$CHD_3(v=0)$ and F+$CHD_3(v_1=1)$ reactions as a function of collision energy. The different binning techniques, HB and GB, are explained in Secs. IV A 1 and IV A 2.

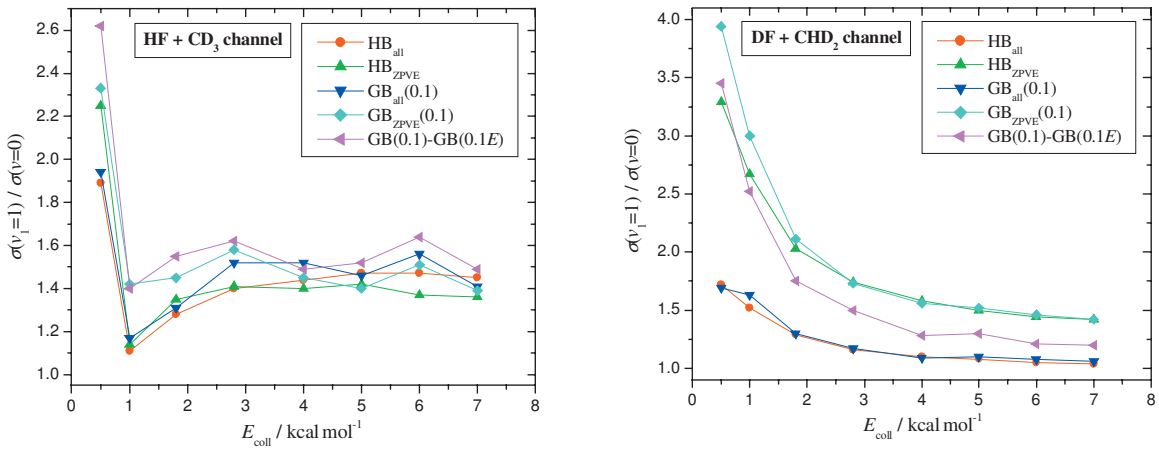

FIG. 4. Ratios of the cross sections of the $F+CHD_3(v_1=1)$ and $F+CHD_3(v=0)$ reactions as a function of collision energy for the channels $HF+CD_3$ and $DF+CHD_2$. The different binning techniques, HB and GB, are explained in Secs. IV A 1 and IV A 2.

and DF; thus in this case HB_{all} means no binning, whereas $GB_{all}(0.1)$ employs a weighted sum over all the reactive trajectories where the weights are based on the diatomic vibrational energies. Here we also consider results where the weight of a trajectory is the product of the diatomic and polyatomic Gaussian weights denoted as GB(0.1)-GB(0.1*E*) (*E* indicates that the polyatomic weight is based on the total vibrational energy [Eq. (13)]).

For the $F+CHD_3(v=0)$ reaction the DF:HF ratio (2.6–2.8 or 1.5–2.5 with ZPVE constrained binnings) is below the statistical value, 3. The ZPVE constrained binning methods give lower ratios since the CHD_2 is more likely to violate the ZPVE than CD_3. The GB(0.1)-GB(0.1*E*) method gives a ratio of about 2.5 with slight E_{coll} dependency. The nonstatistical ratios show that the break of the CH bond is favored relative to the CD bond cleavage. Note that the computation of Espinosa-García employing ZPVE constraint (HB_{ZPVE} with our notation) gave qualitatively similar result, i.e., a DF:HF ratio of 1.72 at $E_{coll}=2.8$ kcal/mol.[21] In the case of the $F+CHD_3(v_1=1)$ reaction the calculations show an increase in the DF:HF ratio over the statistical value of 3 [and over the ratio in the $F+CHD_3(v=0)$ reaction] in the collision energy range of 0.8–1.4 kcal/mol. This unexpected effect of the reactant CH stretch excitation agrees qualitatively with the recent experiment of Zhang *et al.*[7] We have shown in a recent Communication that it is due to the fact that the CH stretching excitation steers the F atom to one of the CD bonds.[23] Note that the ZPVE constraint increases the DF:HF ratios since in the $DF+CHD_2$ channel the methyl product is often CH excited, thus it is unlikely to violate the ZPVE. It is interesting to see that the GB(0.1)-GB(0.1*E*) method supports the ZPVE constrained ratios at low collision energies. The cross section ratios of the $F+CHD_3(v_1=1)$ and $F+CHD_3(v=0)$ reactions are shown in Fig. 4. The CH stretching excitation increases the overall cross sections by factors of about 1.4($HF+CD_3$) and 1.2($DF+CHD_2$) at $E_{coll}>3$ kcal/mol. For the $DF+CHD_2$ channel this ratio tends to 1 at high collision energies (here the ZPVE constraint overestimates the ratio since only the ground state reaction is likely to violate the ZPVE). The CH stretching excitation effect on the $CHD_2(v_1=1):CHD_2(v=0)$ vibrationally state-specific ratios will be discussed in Sec. IV B 3, where we compare the computed results to the measured ones.

3. HF and DF vibrational distributions

The computed normalized vibrational distributions, i.e., $\Sigma_v\langle P_v\rangle=1$, of HF and DF as a function of collision energy are given in Figs. 5 and 6, respectively. In the case of the $F+CHD_3(v=0)$ reaction all the binning techniques show that the most populated HF state is $v=2$ (60%–90%) and the population decreases slightly with increasing collision energy. The fraction of $HF(v=1)$ increases with the collision energy in the range of 10%–20%. The population of $HF(v=3)$ depends significantly on the binning technique employed. For the $HF(v=3)+CD_3$ channel there is an energetic threshold at $E_{coll}=1.5(1.0)$ kcal/mol based on the PES (accurate *ab initio* considering the complete basis set limit, spin-orbit effect, etc.[20]); however, only the $GB_{ZPVE}(\delta)$ results reproduce this behavior. The $GB_{ZPVE}(\delta)$ distributions show that the population of $HF(v=3)$ increases from the threshold at the expense of $HF(v=2)$. The HF distributions of the $F+CHD_3(v_1=1)$ reaction is different from that of the above-discussed ground state reaction since a part of the CH excitation energy of the reactant has been transferred into the HF product resulting in hotter HF vibrational distributions. Indeed, as all the binning techniques show that the population of $HF(v=3)$ rises slightly above $HF(v=2)$ and neither $HF(v=2)$ nor $HF(v=3)$ show significant collision energy dependence in the probability range of 40%–50%. The population of $HF(v=1)$, around 10%, changed only a little with respect to the ground state reaction. Even in the case of the CH stretching excited reaction the $HF(v=4)+CD_3$ channel should be closed at low collision energies, which can be seen on the $GB_{ZPVE}(\delta)$ plot. The other binning techniques, especially HB_{all}, give a small $HF(v=4)$ population even (and erroneously) at low collision energies.

For the $DF(v)+CHD_2$ channel of the $F+CHD_3(v=0)$ reaction the fraction of $DF(v=1)$ is close to zero at low collision energies and rises slowly up to about 10%. The two major states are $DF(v=2)$ and $DF(v=3)$. The population of $DF(v=2)$ increases with the collision energy at the expense

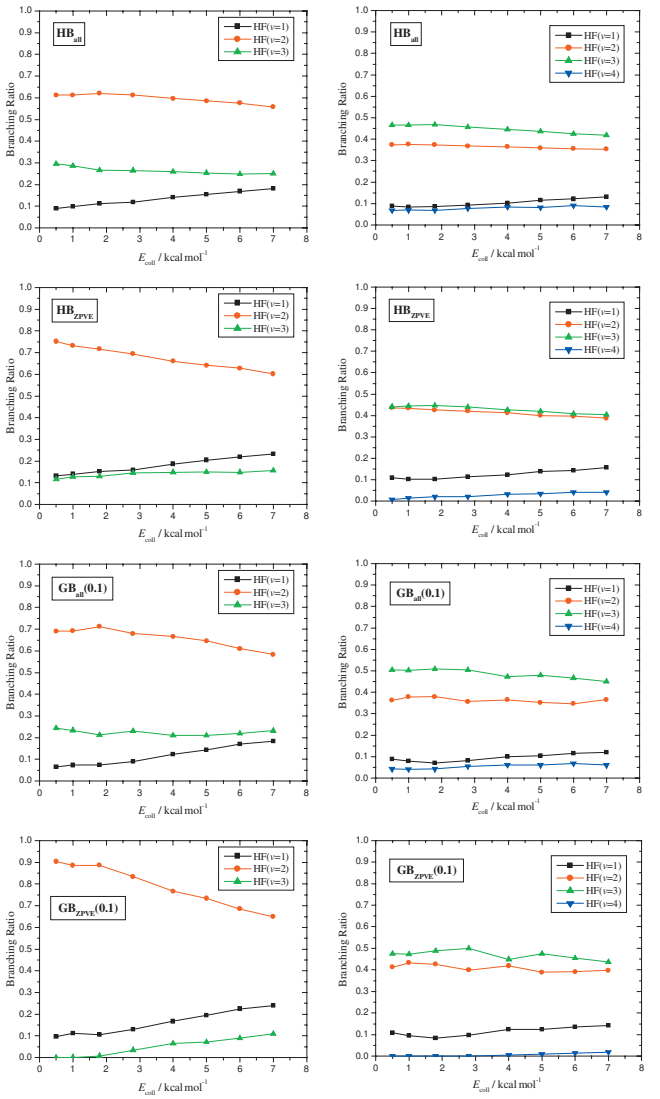

FIG. 5. Normalized HF vibrational populations as a function of collision energy for the reactions F+CHD$_3$(v=0) (left panels) and F+CHD$_3$(v_1=1) (right panels). The different binning techniques, HB and GB, are explained in Sec. IV A 1.

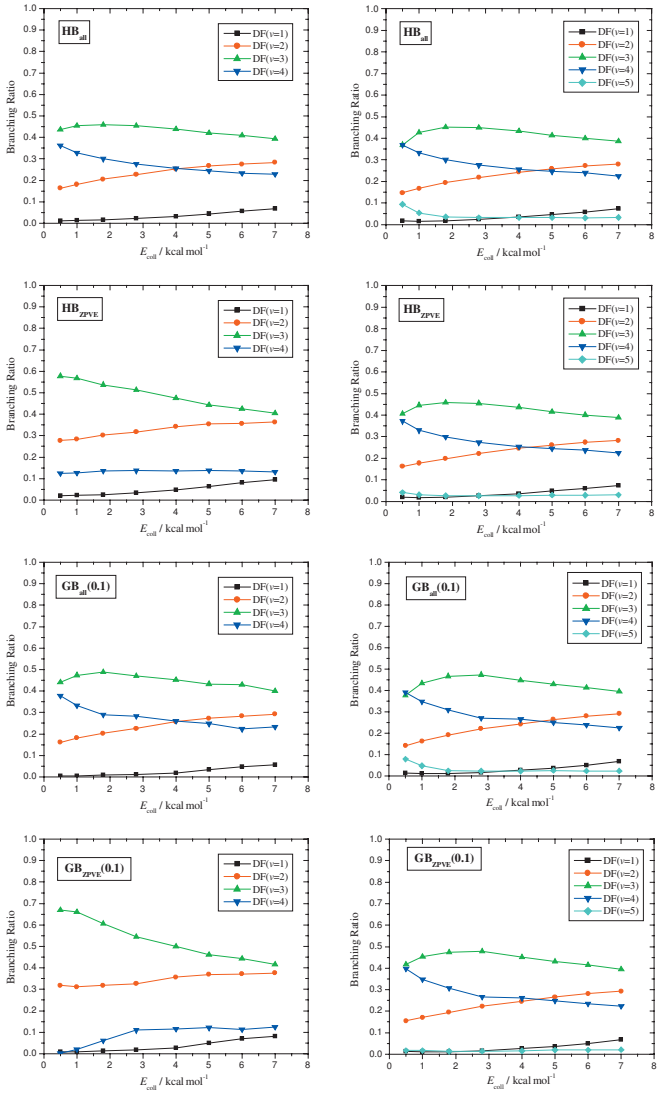

FIG. 6. Normalized DF vibrational populations as a function of collision energy for the reactions F+CHD$_3$(v=0) (left panels) and F+CHD$_3$(v_1=1) (right panels). The different binning techniques, HB and GB, are explained in Sec. IV A 1.

of DF(v=3). At E_{coll}=7 kcal/mol both DF(v=2) and DF(v=3) are close to 40%. All the binning techniques, except GB$_{ZPVE}$(δ), overpopulate DF(v=4). Only GB$_{ZPVE}$(δ) shows a threshold correctly, whose PES (accurate *ab initio*[20]) value is at E_{coll}=0.7(0.3) kcal/mol, and the increase in the relative population of DF(v=4) up to 10%–15%. On the basis of our results the DF(v) distribution of the CH stretching excited reaction does not change significantly relative to the ground state reaction, although the GB$_{ZPVE}$(0.1) plots show an increase in DF(v=4). Note that there is no energetic threshold for DF(v=4) if the CH stretch is excited in the reactant. The similar DF(v) distributions indicate that the CH stretching remains excited in most of the CHD_2 products, thus in most cases the excitation energy of the reactant is not transferred into the DF product. Due to the fact that the most CHD_2 products are vibrationally excited, it is unlikely that the trajectories would violate the ZPVE. Therefore, the ZPVE constrained binning techniques give very similar distributions to the ones obtained by considering all the trajectories.

4. HF and DF rotational distributions

The HF and DF vibrationally state-resolved rotational populations for both reactions, i.e., F+CHD$_3$(v_1=0,1), at collision energy of 1.8 kcal/mol are shown in Fig. 7. Note that each rotational distribution is normalized, i.e., $\Sigma_J\langle P_{v,J}\rangle$ =1 for each v vibrational state of HF or DF. One can generally state for both reactions that both the HF and DF molecules tend to be rotationally colder with the increase in the vibrational excitations. The HF rotational populations corresponding to the F+CHD$_3$(v=0) reaction is very similar to that of the F+CH_4(v=0) reaction.[20] Experimentalists have not probed the HF rotational distribution for the F+CHD$_3$ reaction but measured data are available for the F+CH_4 reaction,[19] where we found excellent agreement between theory and experiment (see Ref. 20). Therefore, we predict that the rotational distributions of the present study could be a realistic guidance and motivation of a future experiment. As expected, the DF(v,J) molecules obtained from the F +CHD$_3$(v=0) reaction are rotationally hotter than the corresponding HF(v,J) products.

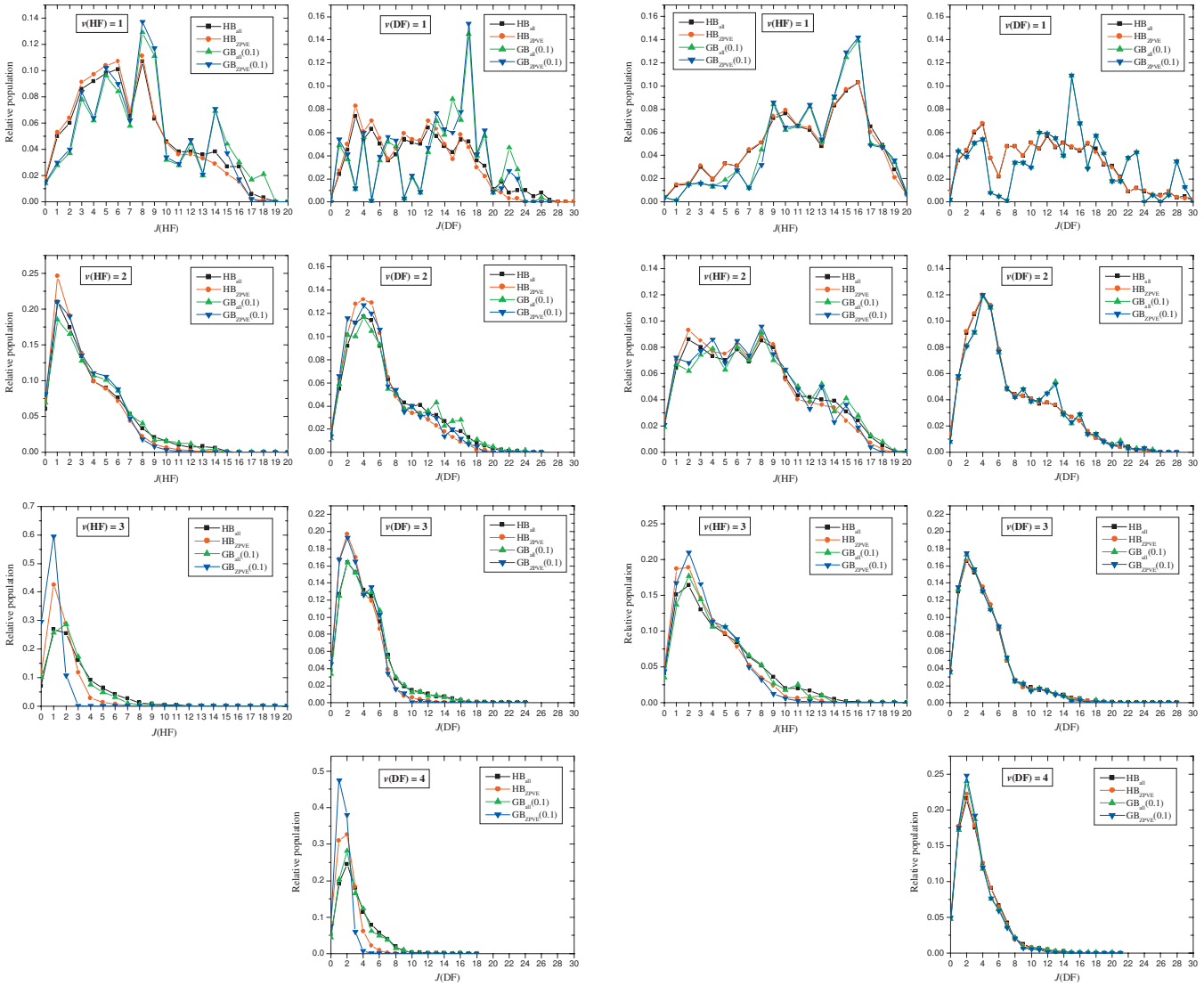

FIG. 7. Normalized HF and DF vibrationally state-resolved rotational populations for the reactions F+CHD$_3$(v=0) (left panels) and F+CHD$_3$(v_1=1) (right panels) at collision energy of 1.8 kcal/mol. The different binning techniques, HB and GB, are explained in Sec. IV A 1.

In the case of the HF channel of the F+CHD$_3$(v_1=1) reaction the QCT results show significantly more rotational excitations relative to F+CHD$_3$(v=0)→HF(v,J)+CD$_3$ reaction. It indicates that the CH excitation energy of CHD$_3$ is not only transferred into HF vibration but also into the rotational degrees of freedom as well. On the other hand the DF rotational distribution corresponding to the F+CHD$_3$(v_1=1) reaction is similar to that of the F+CHD$_3$(v=0) reaction; thus, the CH stretching excitation in the reactant does not cause extra rotational excitations in the DF product.

5. HF and DF angular distributions

The HF and DF vibrationally state-resolved angular distributions are shown in Fig. 8 at the collision energy of 1.8 kcal/mol. All these plots show a preference of the backward scattering for HF/DF(v=1) and the cross sections at the forward directions increase relative to the backward hemisphere with the increase in the HF/DF vibrational excitations. In the case of the F+CHD$_3$(v=0) reaction the HF(v=3) distribution is almost isotropic with a significant peak at forward direction. The DF(v) products of the F+CHD$_3$(v=0) reaction show more contributions in the backward directions than the corresponding HF(v) molecules.

In the case of the CH stretching excited reactant the HF(v) angular distributions show more forward scattering than that of the F+CHD$_3$(v=0) reaction. The HF(v=3) products are mainly forward scattered in the case of the F+CHD$_3$(v_1=1) reaction. Similar to the rotational distributions the DF angular distributions do not change significantly if the CH stretch is excited in the reactant.

We note that the above results are not methyl-state specific. We did present correlated angular distributions for the F+CHD$_3$(v=0)→DF(v)+CHD$_2$(v=0) and F+CHD$_3$(v_1=1)→DF(v)+CHD$_2$(v_1=1) reactions in Ref. 23. All the features discussed above (and shown in Fig. 8) are qualitatively the same considering either the specific CHD$_2$(v=0) and CHD$_2$(v_1=1) states or all the CHD$_2$(v) states. These computed results are in semiquantitative agreement with the measured correlated angular distributions of Liu and co-workers.[7]

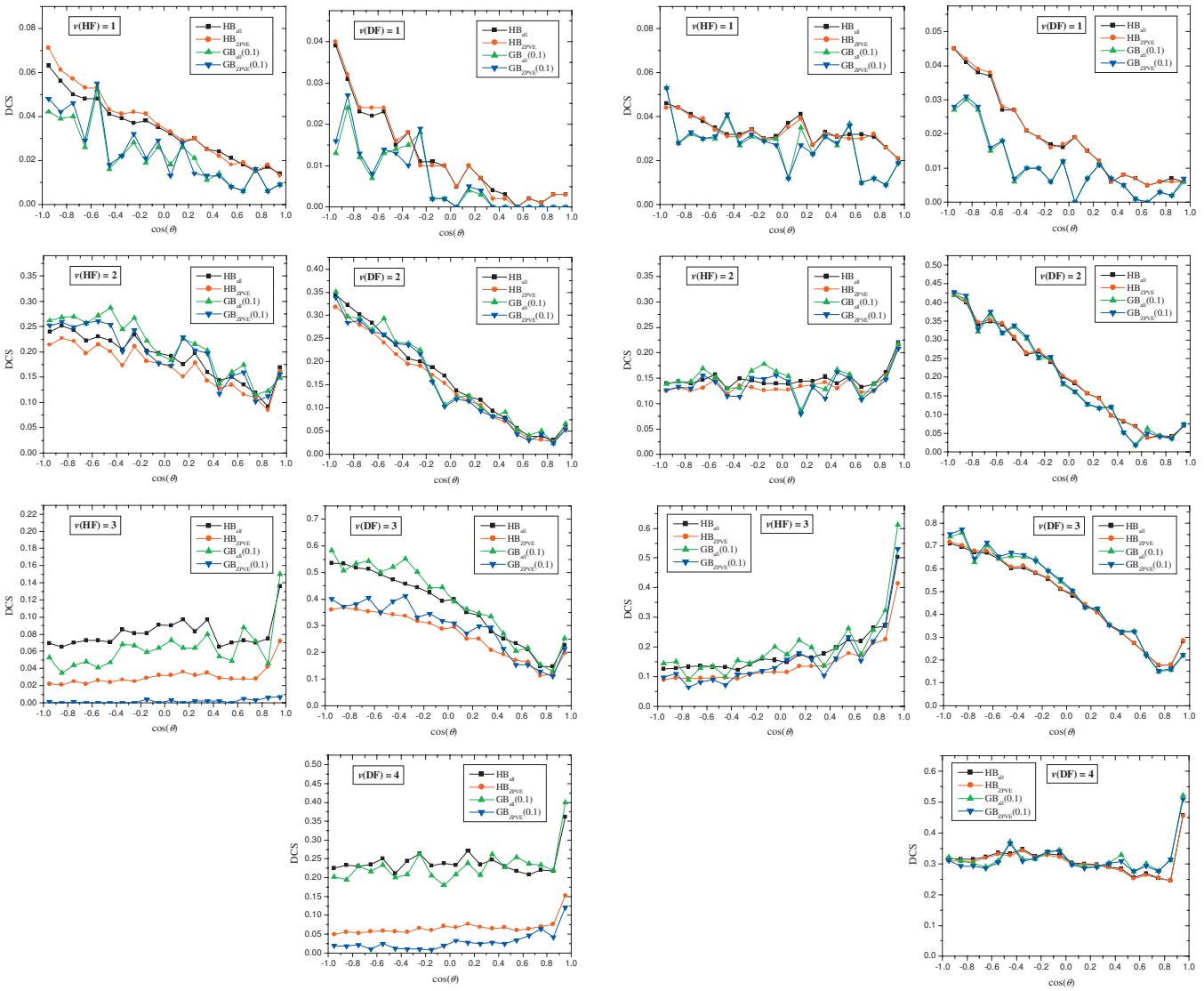

FIG. 8. HF and DF vibrationally state-resolved angular distributions for the reactions F+CHD$_3$(v=0) (left panels) and F+CHD$_3$(v_1=1) (right panels) at collision energy of 1.8 kcal/mol. The different binning techniques, HB and GB, are explained in Sec. IV A 1.

B. Polyatomic product vibrational distributions

1. Binning techniques

The vibrational quantum numbers of the polyatomic products have been assigned, as described in Sec. II. For CD_3 (D_{3h} symmetry) we have determined four quanta ($n_1n_2n_3n_4$), where n_1 and n_2 are the symmetric stretching and out-of-plane bending (umbrella) modes, respectively, whereas n_3 and n_4 are polyad numbers, i.e., sum of two quanta, corresponding to the doubly degenerate stretching and bending modes, respectively. In the case of CHD_2 (C_{2v} symmetry) there is no degeneracy, thus six quanta have been calculated ($n_1n_2n_3n_4n_5n_6$). The most important ones for the present study are n_1 (CH stretching mode) and n_4 (out-of-plane umbrella mode). We employed both HB and GB via the two approaches described in Sec. II B, i.e., GB(δn) and GB(δE). In these notations n and E indicate that the weights are computed for each quanta [Eqs. (11) and (12)] or based on the total vibrational energy [Eq. (13)], respectively. The employed full width at half maximum values were 0.25 and 0.30 for GB(δn) and 0.05 and 0.10 for GB(δE). For example, in the case of GB(δE) δ=0.10 corresponds to 954 and 1070 cm^{-1} for CD_3 and CHD_2, respectively.

2. $CD_3(v)$ *and* $CHD_2(v)$

The vibrational distributions for CD_3 and CHD_2 at different collision energies are given in Tables IV and V, respectively. In the case of the F+CHD$_3$(v=0) reaction the most populated CD_3 states are the ground (9%–23%) and v_2=1 (12%–20%) states. Furthermore, the umbrella overtones v_2=2–4, the $v_4(e')$=1 bending mode (2%–6%), and their combinations have significant populations. The excitation of the stretching modes of CD_3 (v_1 and v_3) is negligible (0%–2%). The picture is similar in the case of the CHD_2 product of the F+CHD$_3$(v=0) reaction, although the ground state is more pronounced (22%–37%) and the v_3=1 in plane bending mode has more population (4%–9%) than the $v_4(e')$ mode of CD_3. The CH stretching mode (v_1) is clearly not excited in the collision energy range investigated; however,

TABLE IV. Vibrational distributions (%) for the CD_3 products of the reactions $F+CHD_3(v=0)$ and $F+CHD_3(v_1=1)$ at eight different collision energies in the 0.5–7.0 kcal/mol range [the normalized populations were obtained by GB(0.30n)].

	$F+CHD_3(v=0)\rightarrow HF+CD_3(n_1n_2n_3n_4)$									$F+CHD_3(v_1=1)\rightarrow HF+CD_3(n_1n_2n_3n_4)$							
$(n_1n_2n_3n_4)$	ω [a]	0.5	1.0	1.8	2.8	4.0	5.0	6.0	7.0	0.5	1.0	1.8	2.8	4.0	5.0	6.0	7.0
(0000)	4769	15	23	9	12	16	18	17	18	10	9	10	12	11	8	11	10
(0010)	2444	0	0	0	0	2	1	1	1	0	2	0	1	1	1	1	1
(1000)	2186	0	0	0	1	0	0	1	0	1	2	1	1	1	1	1	1
(0001)	1036	2	2	5	4	3	4	6	5	5	5	5	6	5	5	4	4
(0100)	394	18	12	16	20	14	16	15	14	5	8	10	10	10	12	8	14
(0200)	788	8	14	19	12	10	11	11	11	5	7	6	7	6	10	8	8
(0300)	1182	8	8	8	7	9	6	8	7	8	6	6	8	8	5	6	8
(0400)	1576	7	7	4	5	4	6	4	5	6	6	4	4	6	5	6	3
(0500)	1970	8	4	3	3	3	6	3	3	7	3	2	3	3	3	4	3
(0600)	2364	2	2	3	1	2	2	2	3	2	1	1	1	2	2	2	2
(1100)	2580	0	1	1	2	1	1	1	1	2	1	0	1	2	1	1	1
(0101)	1430	2	3	5	8	5	4	6	4	3	7	7	3	6	7	6	6
(1200)	2974	0	1	0	0	0	0	1	0	1	0	1	0	1	0	1	0
(0201)	1823	4	5	5	4	6	4	4	6	5	5	4	6	6	4	5	6
(0301)	2217	4	4	5	3	4	6	4	3	4	5	6	4	4	4	5	3
Σ [b]		80	85	84	82	79	85	83	82	64	67	64	67	70	69	70	70

[a]Harmonic frequencies (in cm^{-1}) corresponding to the PES. The overtones and combination bands are the sum of the corresponding harmonic fundamentals. The ω corresponding to (0000) is the harmonic ZPVE and all the other energies are relative to the ZPVE.
[b]Total population of the vibrational states listed here. There are a lot of other open states but each of them has small percentage (usually $\ll 1\%$).

TABLE V. Vibrational distributions (%) for the CHD_2 products of the reactions $F+CHD_3(v=0)$ and $F+CHD_3(v_1=1)$ at eight different collision energies in the 0.5–7.0 kcal/mol range [the normalized populations were obtained by GB(0.30n)].

	$F+CHD_3(v=0)\rightarrow DF+CHD_2(n_1n_2n_3n_4n_5n_6)$									$F+CHD_3(v_1=1)\rightarrow DF+CHD_2(n_1n_2n_3n_4n_5n_6)$							
$(n_1n_2n_3n_4n_5n_6)$	ω [a]	0.5	1.0	1.8	2.8	4.0	5.0	6.0	7.0	0.5	1.0	1.8	2.8	4.0	5.0	6.0	7.0
(000000)	5350	37	23	22	30	24	27	24	23	7	4	3	1	0	1	2	0
(100000)	3227	0	0	0	0	0	0	0	0	9	11	13	14	13	12	15	16
(000010)	2444	0	0	1	1	2	1	2	2	0	1	0	0	0	0	0	0
(010000)	2262	1	3	2	2	2	2	2	1	1	1	1	0	0	0	0	0
(000001)	1291	2	2	2	3	4	4	4	2	2	2	0	1	0	1	1	1
(001000)	1041	4	7	9	6	6	6	6	6	6	1	3	2	0	0	0	0
(000100)	435	19	21	20	15	15	20	17	15	7	3	1	1	0	0	2	0
(000200)	870	6	9	10	11	11	10	10	14	8	2	2	0	1	1	1	1
(000300)	1305	6	6	6	4	8	4	4	7	3	3	2	1	1	0	0	1
(000400)	1740	3	2	2	2	2	2	2	3	4	2	1	1	1	0	1	1
(100001)	4518	0	0	0	0	0	0	0	0	1	1	2	1	3	7	3	3
(101000)	4268	0	0	0	0	0	0	0	0	2	6	5	4	2	4	6	4
(100100)	3662	0	0	0	0	0	0	0	0	3	7	8	10	12	9	10	9
(100200)	4097	0	0	0	0	0	0	0	0	3	5	5	7	5	8	5	6
(100300)	4532	0	0	0	0	0	0	0	0	1	2	2	5	4	4	3	3
(100400)	4967	0	0	0	0	0	0	0	0	2	2	2	2	3	1	1	2
(002000)	2082	1	3	1	2	1	2	3	2	2	1	1	0	1	0	0	0
(102000)	5309	0	0	0	0	0	0	0	0	0	0	0	1	1	1	1	1
(000101)	1726	3	1	2	2	2	2	3	2	1	1	1	1	1	0	0	1
(001100)	1476	5	4	5	4	4	4	5	4	2	2	1	0	0	2	0	0
(100101)	4953	0	0	0	0	0	0	0	0	0	1	2	2	2	1	3	1
(101100)	4703	0	0	0	0	0	0	0	0	0	2	2	2	4	4	4	2
(000201)	2161	0	2	0	1	1	2	1	1	2	1	0	1	1	0	0	0
(001200)	1911	2	3	1	2	1	2	2	2	1	2	1	1	0	0	0	0
(100201)	5388	0	0	0	0	0	0	0	0	0	1	1	0	1	1	1	1
(101200)	5138	0	0	0	0	0	0	0	0	0	1	1	4	1	1	2	2
Σ [b]		88	85	86	86	85	87	82	84	68	63	59	63	58	60	63	55

[a]Harmonic frequencies (in cm^{-1}) corresponding to the PES. The overtones and combination bands are the sum of the corresponding harmonic fundamentals. The ω corresponding to (000000) is the harmonic ZPVE and all the other energies are relative to the ZPVE.
[b]Total population of the vibrational states listed here. There are a lot of other open states but each of them has small percentage (usually $\ll 1\%$).

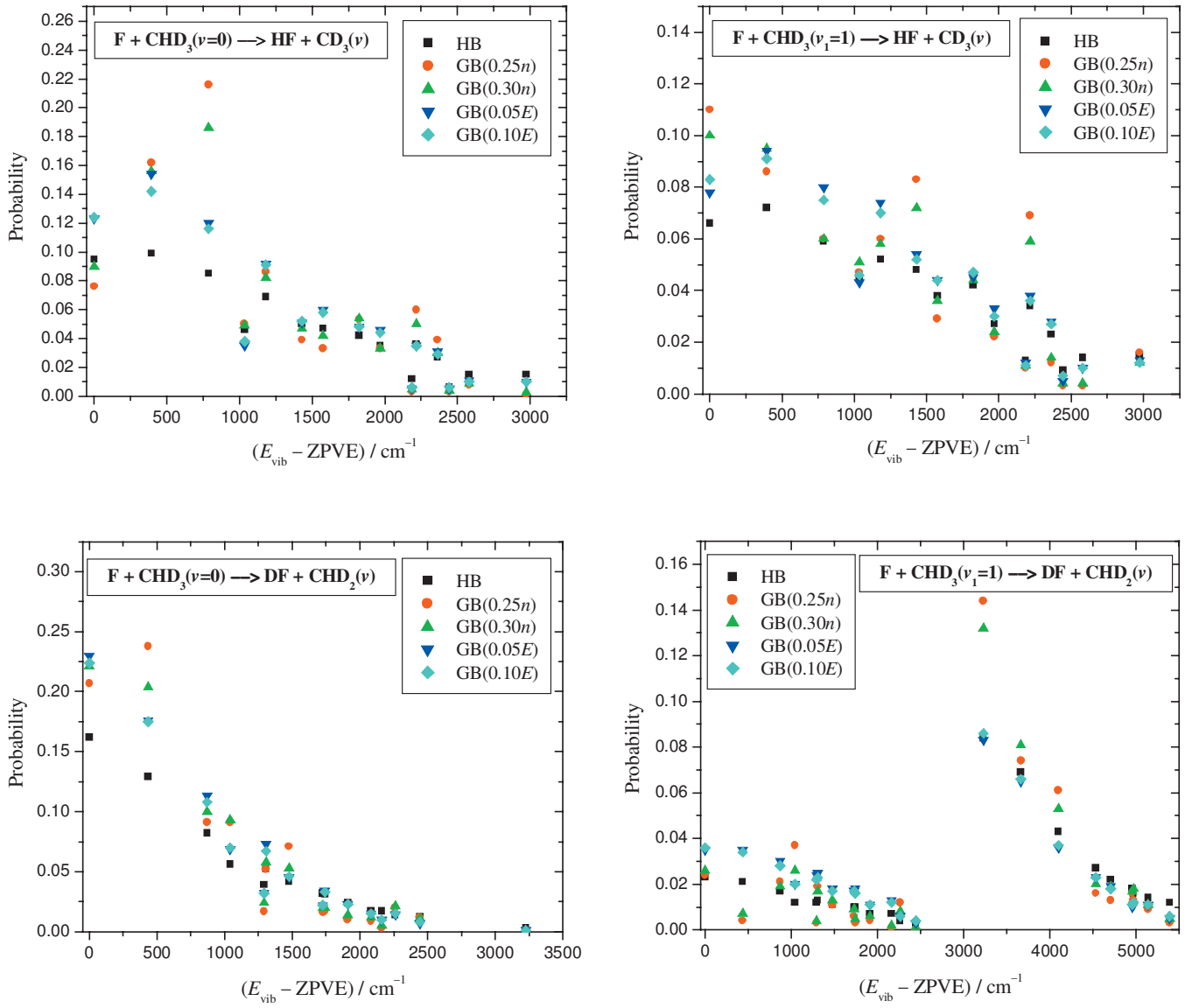

FIG. 9. Normalized vibrational distributions for the CD_3 and CHD_2 products of the reactions F+CHD_3(v=0) (left panels) and F+CHD_3(v_1=1) (right panels) at collision energy of 1.8 kcal/mol. The different binning techniques, HB and GB, are explained in Sec. IV B 1.

the QCT results show small populations for the other two stretching modes v_5 (0%–2%) and v_2 (1%–3%).

Now let us discuss the effect of the CH stretching excitation of the reactant CHD_3 on the polyatomic product vibrational distributions. The vibrational distribution of CD_3 does not change significantly if the v_1 mode of CHD_3 is excited. The populations of the ground state and the umbrella modes of CD_3 slightly decrease, whereas the percentage of the $v_4(e')=1$ in plane bending mode slightly increases especially at low collision energies. The stretching modes are still nonexcited and the populations (0%–2%) are negligible. The case of the DF+CHD_2 channel is completely different. Here we see significant drop in the ground state populations, especially at high collision energies, since in the E_{coll} =1.8–7 kcal/mol range the $CHD_2(v=0)$ populations are 22%–30% and only 0%–3% for the ground state and CH stretching excited reactions, respectively. On the other hand the CH stretching excited $CHD_2(v_1=1)$ molecules appear (9%–16%) if the same mode is excited in the reactant. It is important to note that the other two stretching modes (v_2 and v_5) remain nonexcited (0%–1%), thus we can state that the CH stretching vibrational energy does not leak into the other stretching modes even if they have lower frequencies. The populations of the pure umbrella overtones drop, whereas significant populations appear in the combination bands of the umbrella modes (v_4=1–4) and the CH stretching mode (v_1=1). On the basis of these results it is likely that the CH stretching remains excited in the CHD_2 product, thus the extra vibrational energy is not transferred into the DF vibration. It is important to emphasize that the most populated product state in the F+CHD_3(v_1=1) reaction, especially at higher E_{coll}, is $CHD_3(v_1=1)$, see Table V, in agreement with the experimental results of Liu and co-workers.[7]

The results presented in Tables IV and V were obtained by GB(0.3n). The effects of the choice of different binning techniques have also been tested. Figure 9 shows the CD_3 and CHD_2 vibrational distributions ("spectra") at E_{coll} =1.8 kcal/mol obtained by five different binnings. The HB

usually gives the lowest relative probability for the highly populated states, whereas HB allows small populations ($\ll 1\%$) for many states, which are closed by GB. Figure 9 shows that both HB and GB give the qualitatively same distributions and the different widths used for GB do not result in significant changes in the populations. Based on Fig. 9 some uncertainties can be predicted for the data given in Tables IV and V. Nevertheless, we can be confident that the presented polyatomic vibrational populations and the above conclusions are reasonable.

3. $CHD_2(v_1=1):CHD_2(v=0)$ ratio

The cross section ratio of the reactions $F+CHD_3(v_1=1)\rightarrow DF+CHD_2(v_1=1)$ and $F+CHD_3(v=0)\rightarrow DF+CHD_2(v=0)$ is about 0.3–0.6, i.e., below 1, depending on the binning method, as shown in Ref. 23. Therefore, in the case of these specific product channels the rate of the reaction is slower if the reactant CH stretching mode is excited. This result is in qualitative agreement with experiment, which reports this ratio to be 0.1–0.2.[7] Furthermore, experiment found that the ratio exhibits little collision energy dependency,[7] in good agreement with the present QCT results. However, the computed ratios of cross sections summed over all the CHD_2 states of the excited and ground state reactions are above 1, as shown in Fig. 4. This is due to the fact that the $CHD_2(v=0)$ relative population is higher in the ground state reaction than the $CHD_2(v_1=1)$ population in the CH excited reaction (see Table V).

C. Correlated vibrational distributions

1. Binning techniques

Correlated vibrational quantum numbers have also been computed for $HF(v)+CD_3(n_1n_2n_3n_4)$ and $DF(v)+CHD_2(n_1n_2n_3n_4n_5n_6)$ for both the ground state and CH stretching excited reactions. We have considered the following binning techniques: HB_{HF}-HB_{CD3}, $GB_{HF}(0.1)$-HB_{CD3}, HB_{HF}-$GB_{CD3}(0.1E)$, and $GB_{HF}(0.1)$-$GB_{CD3}(0.1E)$ (and likewise for the other channel). For these correlated binnings we prefer to employ the $GB(\delta E)$ approach [Eq. (13)] instead of $GB(\delta n)$ because this ensures the reasonable statistical error even if GB is used for HF/DF as well. In the case of the $GB_{HF}(0.1)$-$GB_{CD3}(0.1E)$ method the weight of the correlated product pair is obtained by multiplying the diatomic and polyatomic weights.

2. $HF(v)+CD_3(v=0)$ and $DF(v)+CHD_2(v_1=0,1)$

Liu and co-workers[7,9–12] measured the vibrationally state-specific correlation of coincident product pairs in various reactions. In 2004 they published[11] the correlated vibrational branching ratios as a function of collision energy for the $HF(v)+CD_3(v=0)$ and $DF(v)+CHD_2(v=0)$ product channels of the $F+CHD_3(v=0)$ reaction (see Fig. 4 of Ref. 11). Our computed results obtained by employing different binning techniques are shown in Figs. 10 and 11 for the above-mentioned correlated distributions, respectively. Both experiment and theory show that both channels exhibit strong preference for high vibrational states, i.e., $v=2-3$ for HF and $v=3-4$ for DF. The populations of the $v=1$ state of

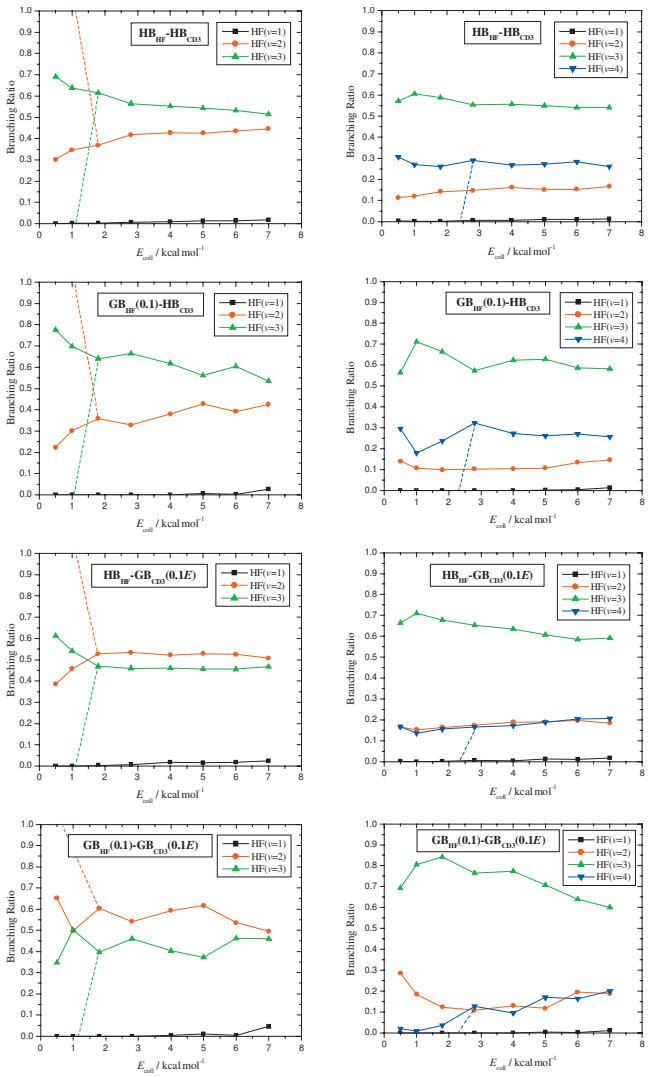

FIG. 10. Correlated $HF(v)+CD_3(v=0)$ vibrational populations as a function of collision energy for the reactions $F+CHD_3(v=0)$ (left panels) and $F+CHD_3(v_1=1)$ (right panels). For the different binning techniques, see Sec. IV C 1. The dashed lines indicate the energetic thresholds, i.e., 1.5 (1.0) and 2.5 (2.4) kcal/mol for $F+CHD_3(v_1=0,1)\rightarrow HF(v=3,4)+CD_3(v=0)$, respectively, corresponding to the PES (accurate *ab initio*).

HF and DF increase slightly with the collision energy and the relative population is just still about 1% at 7 kcal/mol. The $DF(v=2)+CHD_2(v=0)$ relative population has also a slight increase from $E_{coll}=1-2$ kcal/mol and goes up to about 15%–20% at 7 kcal/mol. In the case of this $DF(v=2)$ channel the QCT results are in excellent agreement with experiment.[11] For the $HF(v)+CD_3(v=0)$ channel the measured vibrational branching ratios show a threshold for $HF(v=3)$ at about 1 kcal/mol, then $HF(v=3)$ increases rapidly from the threshold at the expense of $HF(v=2)$ and there is a population inversion between $E_{coll}=1-2$ kcal/mol. $HF(v=3)$[$HF(v=2)$] has a maximum (minimum) at about $E_{coll}=2$ kcal/mol and at higher collision energies the $HF(v=3)$ and $HF(v=2)$ curves tend to slowly approach each other. The QCT plots show high sensitivity for the binning technique employed for the $HF(v=2)+CD_3(v=0)$ and $HF(v=3)+CD_3(v=0)$ product pairs. HB_{HF}-HB_{CD3} and $GB_{HF}(0.1)$-HB_{CD3} methods give almost good results at

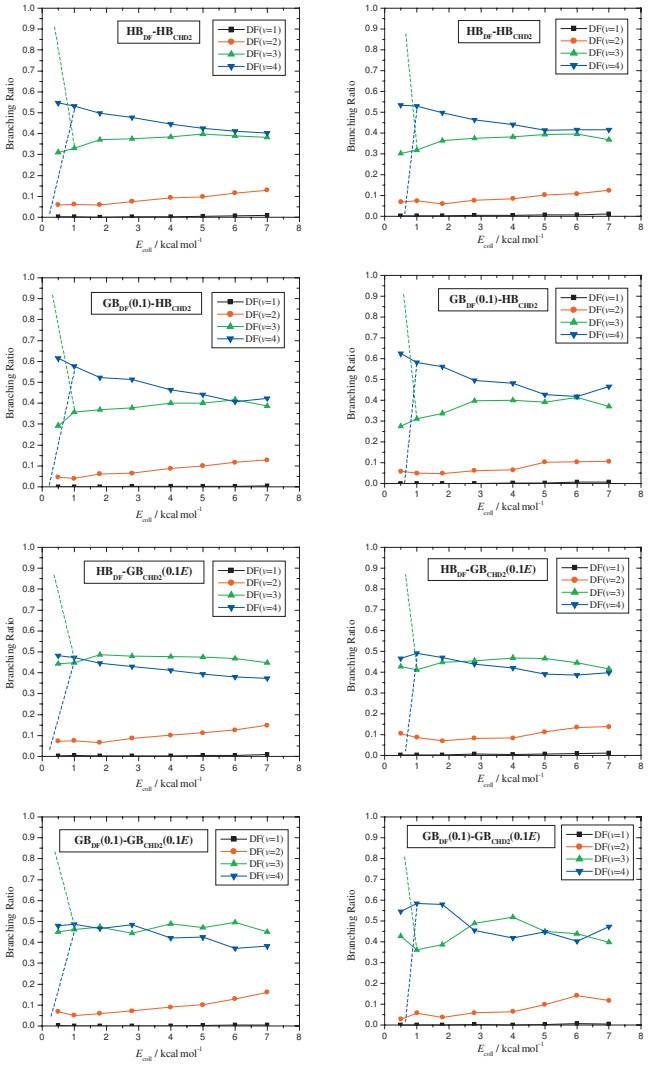

FIG. 11. Correlated DF(v)+CHD$_2$(v=0) (left panels) and DF(v) +CHD$_2$(v_1=1) (right panels) vibrational populations as a function of collision energy for the reactions F+CHD$_3$(v=0) (left) and F+CHD$_3$(v_1=1) (right), respectively. For the different binning techniques, see Sec. IV C 1. The dashed lines indicate the energetic thresholds, i.e., 0.7 (0.3) and 1.0 (0.6) kcal/mol for F+CHD$_3$(v_1=0,1)→DF(v=4)+CHD$_2$(v_1=0,1), respectively, corresponding to the PES (accurate *ab initio*).

higher collision energies, i.e., HF(v=3)>HF(v=2) and HF(v=3) decreases with the collision energy. However, these binning techniques do not reproduce the threshold of HF(v=3) at low collision energies because HB$_{CD3}$ allows the ZPVE violation for CD$_3$(v=0). Only the GB$_{HF}$(0.1)-GB$_{CD3}$(0.1E) binning shows a slight decay of HF(v=3) at low collision energy although the population of HF(v=3) does not rise above that of HF(v=2).

In the case of the DF(v)+CHD$_2$(v=0) channel the measured relative population of v=4(3) is 10(85)% at about E_{coll}=0.5 kcal/mol, then v=4(3) increases (decreases) rapidly and the population is 70% (30%) at around E_{coll} =1 kcal/mol. At E_{coll}>1 kcal/mol, v=4 decreases and crosses the increasing v=3 at E_{coll}=3–4 kcal/mol. The DF(v=3) ratio rises between 1 kcal/mol (30%) and 5 kcal/mol (50%) and decreases if E_{coll}>5 kcal/mol. The computed results cannot reproduce this complicated collision energy dependence shown by experiment. Nevertheless, theory gives that both DF(v=3) and DF(v=4) are between 30% and 60% in a wide collision energy range which agrees with a simplified picture of the experiment.

Recently Zhang *et al.*[7] measured the correlated DF(v) +CHD$_2$(v_1=1) product pairs in the F+CHD$_3$(v_1=1) reaction in the E_{coll}=0.5–3.6 kcal/mol range. The computed results are given in Fig. 11 in a wider collision energy range (0.5–7 kcal/mol). Both experiment and theory show that the DF(v) vibrational ratios are almost the same for the ground state and the CH stretching excited reaction. This can be expected since the harmonic (anharmonic) CH stretching v_1 fundamentals (in cm^{-1}) of CHD$_3$ and CHD$_2$ are 3120 (2985) and 3227 (3097), respectively. Due to the fact that the v_1 fundamentals of the reactant and the CHD$_2$ product are the same within <0.5 kcal/mol and the DF vibrational distributions are correlated with CHD$_2$(v=0) and CHD$_2$(v_1=1) for the F +CHD$_3$(v=0) and F+CHD$_3$(v_1=1) reactions, respectively, the available energy for DF vibrational excitation is almost the same in the two reactions. It is important to note because it is less predictable that we found similar DF vibrational distributions for both reactions even if the DF(v) populations are not correlated with CHD$_2$(v=0) and CHD$_2$(v_1=1) for the corresponding reactions.

The correlated relative vibrational populations for the HF(v)+CD$_3$(v=0) channel of the F+CHD$_3$(v_1=1) reaction are presented in Fig. 10. As expected, we see more vibrational excitations for HF relative to the ground state reaction. For the ground state reaction HF(v=4) is closed over the whole collision energy range investigated, but in the case of the F+CHD$_3$(v_1=1) reaction the HF(v=4)+CD$_3$(v=0) channel opens. However, there is an energetic threshold for HF(v=4)+CD$_3$(v=0) at collision energy of 2.5 (2.4) kcal/mol corresponding to the PES (accurate *ab initio* estimate[20]). The GB$_{HF}$(0.1)-GB$_{CD3}$(0.1E) is the only binning technique which shows a threshold (around 1–2 kcal/mol), thus this is an example again for the utility of the GB method.

3. HF(v) and DF(v) correlated with umbrella mode excited CD$_3$ and CHD$_2$

Figure 12 shows the HF(v) and DF(v) vibrational populations correlated with the umbrella mode excited CD$_3$ and CHD$_2$, respectively, for the F+CHD$_3$(v_1=0,1) reactions at 2.8 kcal/mol collision energy. All the plots show anticorrelation between the vibrational excitations of the coincident product pairs. Similar anticorrelation was observed in the experimental study of the F+CD$_4$(v=0)→DF(v)+CD$_3$(v_2) reaction.[12] In the case of the HF(v)+CD$_3$(0$n_2$00) channel one can see vibrationally hotter HF molecules if the reactant CH stretching mode is excited. For the DF+CHD$_2$ channel the DF(v) distributions are almost the same if they are correlated with CHD$_2$(000$n_4$00) and CHD$_2$(100$n_4$00) for the F +CHD$_3$(v=0) and F+CHD$_3$(v_1=1) reactions, respectively. The results show again that if the excited CH stretch remains excited in the CHD$_2$ product, there is no significant effect of the reactant CH stretching excitation on the vibrational distribution of DF.

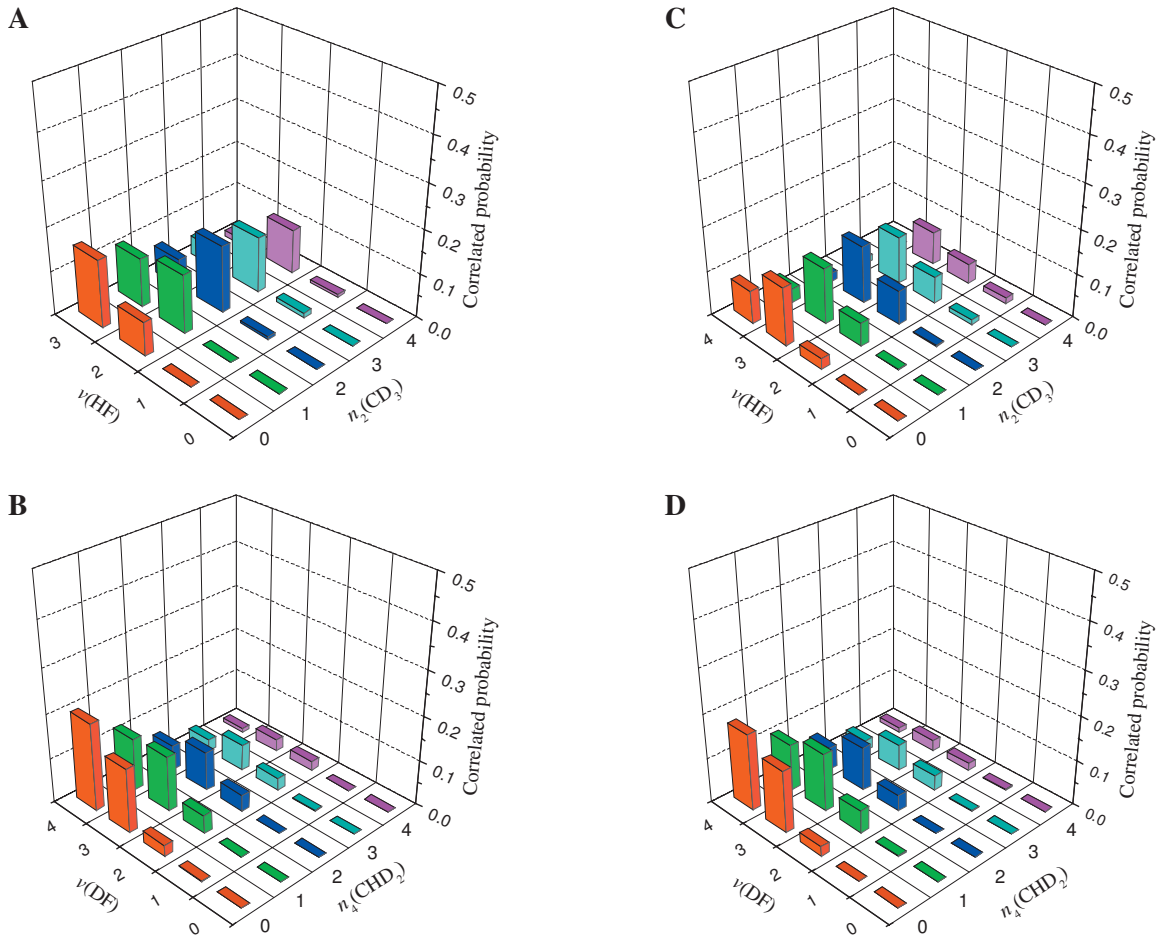

FIG. 12. Correlated HF(v)+CD_3($0n_2$00) (a) and DF(v)+CHD_2(000$n_4$00) (b) vibrational populations for the F+CHD_3(v_1=0) reaction and HF(v)+CD_3($0n_2$00) (c) and DF(v)+CHD_2(100$n_4$00) (d) vibrational populations for the F+CHD_3(v_1=1) reaction at collision energy of 2.8 kcal/mol. The n_2 and n_4 are the umbrella modes for CD_3 and CHD_2, respectively. In panel (d) the n_1 CH stretching mode of CHD_2 is excited. The QCT results were obtained by $GB_{HF/DF}(0.1)$-$HB_{CD3/CHD2}$ (for more details, see Sec. IV C 1).

V. SUMMARY AND CONCLUSIONS

Extensive QCT calculations have been reported for the F+CHD_3(v_1=0,1)→HF(v,J)+CD_3(v) and DF(v,J)+CHD_2(v) reactions using a recent high-quality *ab initio* PES (Ref. 20) and the results have been compared to recent crossed molecular beam experiments.[7,11] Normal mode analysis for the polyatomic products were performed and "quantized" product state distributions were obtained using standard HB and a modification of GB.[27] We have shown that GB can be especially useful at the regions near to the energetic threshold of certain product states. For example, in the case of the F+CHD_3(v_1=1) reaction the HF(v=4)+CD_3(v=0) channel should be closed at E_{coll} <2.5 kcal/mol. The frequently used HB cannot reproduce this energetic threshold, whereas the GB gives the correct behavior. Thus, the use of GB is a promising way to prevent the computation of finite probabilities for energetically not accessible product channels, which is a well-known issue of the standard HB (usually used in QCT product analysis). The most important results of the present study on the dynamics of the title reaction can be summarized as follows.

(1) Both HF and DF products are formed in population inversion, as expected. The most populated vibrational states are HF(v=2) and DF(v=3) for the F+CHD_3(v=0) reaction and HF(v=3) and DF(v=3) for the F+CHD_3(v_1=1) reaction. The reactant CH stretching excitation does not change the DF vibrational distribution significantly.

(2) The branching ratio for DF:HF for the ground state reaction varies roughly 1.5–2.8 depending the binning method and collision energy. Therefore, in the case of the F+CHD_3(v=0) reaction the abstraction of the H atom is slightly promoted since the DF:HF ratio is below the statistical value of 3. On the other hand in the case of the F+CHD_3(v_1=1) reaction we found a significant enhancement for the D abstraction over the H abstraction at low collision energies. The DF:HF ratio is about twice as large as that in the ground state reaction at around E_{coll}=1 kcal/mol. This unexpected behavior agrees with the recent experiment of Liu and co-workers[7] and it is due to the fact that the CH stretching excitation steers the F atom to the CD bond at low collision energies. For more details the interested reader should consult Ref. 23.

(3) The HF/DF vibrationally state-specific rotational distributions tend colder with increasing vibrational excitations. In the case of the F+CHD_3(v=0) reaction the rotational distribution for HF(v=1) is broad in the

range $J=0-20$ with a maximum at $J=8$, whereas for HF($v=2$) and HF($v=3$) it has a sharp peak at $J=1$ and after a fast decay, it tends to vanish at about $J=14$ and $J=8$, respectively. As expected, the DF rotational distributions are significantly hotter than those of the HF molecules in the case of the F+CHD$_3$($v=0$) reaction. The reactant CH stretching excitation produces rotationally hotter HF molecules, i.e., HF($v=1,J$) peaks at $J=16$, while HF($v=2,J$) and HF($v=3,J$) are similar to HF($v=1,J$) and HF($v=2,J$) of the ground state reaction, respectively. On the other hand the effect of the CH stretching excitation on the DF rotational distributions is insignificant. Therefore, unlike for the ground state reaction in the case of the F+CHD$_3$($v_1=1$) reaction, the HF(v,J) molecules are rotationally roughly as hot as the DF(v,J) products.

(4) The HF/DF vibrationally state-resolved angular distributions show backward scattering at small v, and more and more molecules appear at the forward directions with increasing v. The reactant CH stretch excitation changes the HF angular distributions, whereas it has only slight effect on the DF scattering angles.

(5) The CD$_3$(v) vibrational distributions are similar for the ground and CH stretch excited reactions. Note that the HF(v) distributions are different. The CD$_3$($v=0$) and the umbrella excited CD$_3$($v_2=1$) product states have the highest populations. In the case of CHD$_2$(v) the ground state reaction produces mostly CHD$_2$($v=0$) products, whereas the reactant CH stretch excitation results in mainly CH stretch excited CHD$_2$($v_1=1$) molecules and the fraction of CHD$_2$($v=0$) drops. The dominance of CHD$_2$($v_1=1$) agrees with the recent experiment.[7]

(6) Considering the HF(v)+CD$_3$($v=0$) correlated vibrational distributions the conclusion is similar to that of the HF(v) results, i.e., the CH stretch excitation increases the population of HF($v=3$) relative to that of HF($v=2$). Furthermore, the reactant CH stretching excitation opens the HF($v=4$)+CD$_3$($v=0$) channel, which is energetically not accessible in the ground state reaction. The correlated DF(v)+CHD$_2$($v=0$) and DF(v)+CHD$_2$($v_1=1$) product distributions of the reactions F+CHD$_3$($v=0$) and F+CHD$_3$($v_1=1$), respectively, are similar and the two major diatomic product states are DF($v=3$) and DF($v=4$).

(7) The correlated results for HF(v)+CD$_3$(v_2) and DF(v)+CHD$_2$(v_4) show the anticorrelation between the vibrational excitations of diatomic molecule and methyl umbrella mode.

Finally, we note that our computed anharmonic HF vibrational fundamental of the vdW complex $(CD_3-HF)_{vdW}$ is 3773 cm^{-1} in good agreement with experiment (3787 cm^{-1}).[39] The computed (measured) redshifts of this frequency relative to the same bands of $(CH_3-HF)_{vdW}$ and HF monomer are 13 (10) and 168 (174) cm^{-1}, respectively. Furthermore, we have predicted an anharmonic frequency of 2784 cm^{-1} for the DF stretching fundamental of $(CHD_2-DF)_{vdW}$, redshifted by 104 cm^{-1} relative to the DF monomer, which has not been measured yet.

ACKNOWLEDGMENTS

Discussions with Dr. Kopin Liu on their current experiments are gratefully acknowledged. We also thank Dr. Bas Braams for his valuable comments on the normal mode analysis. We acknowledge that this work was partially conducted under the auspices of the iOpenShell Center for Computational Studies of Electronic Structure and Spectroscopy of Open-Shell and Electronically Excited Species supported by the National Science Foundation through the CRIF:CRF Grant No. CHE-0625237. Financial support from the Department of Energy (Grant No. DE-FG02-97ER14782) is also acknowledged.

[1] J. C. Polanyi, Science **236**, 680 (1987).
[2] S. Yoon, R. J. Holiday, and F. F. Crim, J. Phys. Chem. B **109**, 8388 (2005).
[3] R. J. Holiday, C. H. Kwon, C. J. Annesley, and F. F. Crim, J. Chem. Phys. **125**, 133101 (2006).
[4] S. Yan, Y.-T. Wu, B. Zhang, X.-F. Yue, and K. Liu, Science **316**, 1723 (2007).
[5] H. A. Bechtel, Z. H. Kim, J. P. Camden, and R. N. Zare, J. Chem. Phys. **120**, 791 (2004).
[6] H. A. Bechtel, J. P. Camden, D. J. A. Brown, and R. N. Zare, J. Chem. Phys. **120**, 5096 (2004).
[7] W. Zhang, H. Kawamata, and K. Liu, Science **325**, 303 (2009).
[8] T. Xie, J. M. Bowman, J. W. Duff, M. Braunstein, and B. Ramachandran, J. Chem. Phys. **122**, 014301 (2005).
[9] W. Shiu, J. J. Lin, K. Liu, M. Wu, and D. H. Parker, J. Chem. Phys. **120**, 117 (2004).
[10] W. Shiu, J. J. Lin, and K. Liu, Phys. Rev. Lett. **92**, 103201 (2004).
[11] J. Zhou, J. J. Lin, and K. Liu, J. Chem. Phys. **121**, 813 (2004).
[12] J. J. Lin, J. Zhou, W. Shiu, and K. Liu, Science **300**, 966 (2003).
[13] H. Kornweitz, A. Persky, and R. D. Levine, Chem. Phys. Lett. **289**, 125 (1998).
[14] D. Troya, J. Millan, I. Banos, and M. González, J. Chem. Phys. **120**, 5181 (2004).
[15] J. F. Castillo, F. J. Aoiz, L. Banares, E. Martinez-Nunez, A. Fernandez-Ramos, and S. Vazquez, J. Phys. Chem. A **109**, 8459 (2005).
[16] D. Troya, J. Chem. Phys. **123**, 214305 (2005).
[17] O. Roberto-Neto, F. B. C. Machado, and F. R. Ornellas, Chem. Phys. **315**, 27 (2005).
[18] J. Espinosa-García, J. L. Bravo, and C. Rangel, J. Phys. Chem. A **111**, 2761 (2007).
[19] W. W. Harper, S. A. Nizkorodov, and D. J. Nesbitt, J. Chem. Phys. **113**, 3670 (2000).
[20] G. Czakó, B. C. Shepler, B. J. Braams, and J. M. Bowman, J. Chem. Phys. **130**, 084301 (2009).
[21] J. Espinosa-García, Chem. Phys. Lett. **454**, 158 (2008).
[22] J. Espinosa-García and J. L. Bravo, J. Phys. Chem. A **112**, 6059 (2008).
[23] G. Czakó and J. M. Bowman, J. Am. Chem. Soc. **131**, 17534 (2009).
[24] W. L. Hase, *Encyclopedia of Computational Chemistry* (Wiley, New York, 1998), pp. 399–407.
[25] G. C. Schatz, *Molecular Collision Dynamics*, edited by J. M. Bowman (Springer-Verlag, Berlin, 1983), pp. 25–60.
[26] C. Eckart, Phys. Rev. **47**, 552 (1935).
[27] L. Bonnet and J. C. Rayez, Chem. Phys. Lett. **277**, 183 (1997).
[28] L. Bonnet and J. C. Rayez, Chem. Phys. Lett. **397**, 106 (2004).
[29] L. Bañares, F. J. Aoiz, P. Honvault, B. Bussery-Honvault, and J.-M. Launay, J. Chem. Phys. **118**, 565 (2003).
[30] M. L. González-Martínez, W. Arbelo-González, J. Rubayo-Soneira, L. Bonnet, and J. C. Rayez, Chem. Phys. Lett. **463**, 65 (2008).
[31] B. J. Braams and J. M. Bowman, Int. Rev. Phys. Chem. **28**, 577 (2009).
[32] MOLPRO, a package of *ab initio* programs written by H.-J. Werner, P. J. Knowles, R. Lindh *et al.*, see http://www.molpro.net.

[33] S. Carter, J. M. Bowman, and N. C. Handy, Theor. Chem. Acc. **100**, 191 (1998).
[34] J. M. Bowman, S. Carter, and X. Huang, Int. Rev. Phys. Chem. **22**, 533 (2003).
[35] J. K. G. Watson, Mol. Phys. **15**, 479 (1968).
[36] J. O. Jung and R. B. Gerber, J. Chem. Phys. **105**, 10332 (1996).
[37] S. Carter, S. J. Culik, and J. M. Bowman, J. Chem. Phys. **107**, 10458 (1997).
[38] G. Czakó, B. J. Braams, and J. M. Bowman, J. Phys. Chem. A **112**, 7466 (2008).
[39] J. M. Merritt, S. Rudić, and R. E. Miller, J. Chem. Phys. **124**, 084301 (2006).
[40] T. Shimanouchi, NIST Standard Reference Database 69, Tables of Molecular Vibrational Frequencies Consolidated Vol. I, National Bureau of Standards, p. 1 (1972).
[41] J. L. Brum, R. D. Johnson III, and J. W. Hudgens, J. Chem. Phys. **98**, 3732 (1993).
[42] E. A. Shenyavskaya and V. S. Yungman, J. Phys. Chem. Ref. Data **33**, 923 (2004).
[43] R. N. Spanbauer and K. N. Rao, J. Mol. Spectrosc. **16**, 100 (1965).